Reprint from
Topics in Current Physics
Volume 30: **Real-Space Renormalization**
Editors: T. W. Burkhardt and J. M. J. van Leeuwen

Springer-Verlag
Berlin Heidelberg New York

Real-Space Renormalization

Editors: T. W. Burkhardt and J. M. J. van Leeuwen

7. Position-Space Renormalization Group for Models of Linear Polymers, Branched Polymers, and Gels

H. E. Stanley[1], P. J. Reynolds[2], S. Redner, and F. Family[3]

With 15 Figures

In this chapter we describe how position-space renormalization group methods can be used to treat models of linear polymers, branched polymers, and gels. Apart from their increasingly widespread use to describe phenomena occurring in polymeric systems, these models are of great interest in their own right, since they are purely geometric models embodying the full richness of ordinary thermal critical phenomena.

The organization of this chapter is as follows. Section 7.1 describes the three physical systems that are the principal focus of this review. In Sect.7.2, we describe three mathematical models that have proved useful in capturing the essential physics of the corresponding polymeric systems. Section 7.3 is devoted to a somewhat pedagogical description of how position-space renormalization group methods can be applied to each model. Finally, in Sects.7.4,5, we briefly describe additional approaches and draw some general conclusions.

Our aim is a self-contained exposition of some of the basic ideas rather than a comprehensive review of all work on this subject. Indeed, the application of modern methods of statistical mechanics to polymers is such a rapidly expanding field that it would be impossible to set higher goals for this chapter. For a recent authoritative monograph on polymer physics, see e.g., [7.1].

7.1 Three Physical Systems

7.1.1 Linear Polymers

In this section we introduce three basic classes of polymeric systems. Polymers are macromolecules which form by the chemical bonding of many monomeric constituents. A typical number for the "degree of polymerization" is about 10^4. On the other hand, the number of particles in a system (such as a fluid) exhibiting ther-

---

[1] John Simon Guggenheim Memorial Fellow, 1980- 1981.
[2] Also at MMRD, Lawrence Berkeley Lab, Univ. of California, Berkeley, CA 94720.
[3] Present address: Department of Physics, Center for Polymer Studies, Emory University, Atlanta, GA 30322. Supported in part by grants from ARO, ONR, and NSF.

mal critical phenomena is upwards of 10^{20}. Fortunately, it turns out that even for a polymer with "only" 10^4 monomers, statistical mechanics is a useful and highly appropriate tool.

Suppose, for simplicity, that all the monomers are identical, each having f functional groups which can react with one of the f groups of another monomer. The functionality is important in determining the topological structure of the resulting polymer. The simplest case, f = 0, produces no reactions at all; an example might be argon. The next simplest case, f = 1, results in dimers only. If f = 2, however, we are able to form unbranched linear polymers (Fig.7.1a).

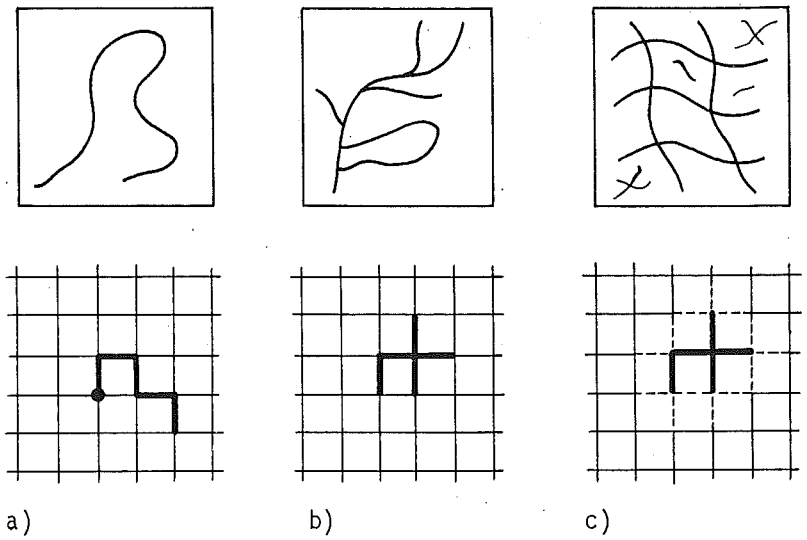

Fig.7.1a-c. Schematic illustration of the three polymeric systems and the lattice models used to describe their asymptotic or "critical" properties, (a) a linear polymer, modeled by an SAW, (b) a branched polymer, modeled by a random lattice animal, and (c) polyfunctional condensation (gelation), modeled by bond percolation. Specifically, (a) shows anL-step SAW whose global nonintersection constraint models the excluded volume effect for linear polymers in a good solvent. (b) shows anL-bond lattice animal, i.e., a connected L-bond cluster, which models a single branched polymer. This represents a generalization of an SAW in that branching can occur. Finally, (c) illustrates a single L-bond percolation cluster (actually many such clusters occur, cf. Fig.7.4). Such clusters are identical to lattice animals, but their relative probabilities of occurrence are different. All random animals with the same number of bonds are equally probable, while percolation clusters are weighted by an additional factor for each perimeter bond (----). In this figure, L is chosen to be 5 for the sake of simplicity only; in actual calculations, L might be as large as 10^2-10^6

Perhaps the most important physical feature of a polymer is the "excluded-volume" effect: the physical fact that two different monomers cannot occupy the same spatial position. For the case of a linear polymer this constraint means that the chain is non-Markovian in nature; hence it cannot be adequately described by a purely random-walk model.

One fundamental geometric property used to characterize a polymer chain in dilute solution is its mean end-to-end distance ξ. There has been considerable work in trying to understand the asymptotic dependence of ξ on the molecular weight M. This behavior is characterized by a critical exponent ν, defined by

$$\xi \sim M^{\nu} \quad [M \to \infty] \quad . \tag{7.1}$$

A simple approach for linear polymers, due originally to FLORY [7.2], has proved to be remarkably successful. This approach is based on minimizing the free energy of a polymer chain within a mean-field approximation. It leads to [7.3]

$$\nu_F = 3/(d + 2) \quad (d \leq 4) \quad , \tag{7.2}$$

where d is the spatial dimension of the system [7.1]. This simple formula is exact for d = 1 and d = 4, and appears to be a very accurate approximation for d = 2 and d = 3 as well. Above four dimensions, the Flory theory predicts that the chain is Gaussian, so that $\nu = 1/2$.

The intriguing simplicity and remarkable accuracy of (7.2) has stimulated considerable work on understanding the underlying basis of the Flory theory [7.1]. Although the physical arguments leading to (7.2) are mean field in character, the apparent reason for the high degree of accuracy is a delicate cancellation of errors in the energy and entropy terms in the Flory free energy [7.1,4]. However, an exact expansion for ν in the quantity (4-d) disagrees with (7.2) already at first order [7.5]. An expansion in (d-1), which may also be exact, also disagrees with (7.2) at first order, as we shall discuss in Sect.7.3.2.

Further interest in understanding linear polymers in dilute solution stems from the discovery of a correspondence between this system and the n-vector model of ferromagnetism [7.6] in the $n \to 0$ limit [7.5,7]. In this correspondence, it turns out that the variable M^{-1} in the polymer system corresponds to the variable $T - T_c$ in the magnetic system. Thus the limit of large molecular weight corresponds to a second-order phase transition. As a result, one expects quantities such as the polymer "diameter" to be characterized by universal behavior. In addition, the existence of a phase transition allows one to apply such modern techniques as the renormalization group to study the polymer problem.

7.1.2 Branched Polymers

The above remarks on linear polymers are readily generalized to more complicated structures. For example, if the constituent monomers have three or more functional groups ($f \geq 3$), we can form branched polymers as illustrated schematically in Fig. 7.1b.

Do we expect branched polymers to obey the same physical laws as linear polymers? Indeed the same "scaling law," (7.1), *is* obeyed for branched polymers, but the critical exponent ν is different.[1] The Flory theory for linear polymers can be gener-

Footnote 1 see next page

alized with the result [7.8-9]

$$\nu = 5/[2(d + 2)] \quad (d \leq 8) \quad . \tag{7.3}$$

In contrast to the case of linear polymers, (7.3) gives the exact result for d = 3 [7.10] and d = 8 [7.11,12], and seems very accurate in d = 2. Moreover, while the magnetic analog of the linear polymer is the n → 0 limit of the n-vector model, the magnetic analog of the branched polymer is somewhat more complicated [7.11,13-15]. Table 7.1 compares the basic scaling properties of linear and branched polymers.

Table 7.1. Comparison of some of the "scaling" properties of (a) linear polymers, (b) branched polymers, and (c) gels. The first line gives d_c, the upper marginal dimension. The second line gives the critical exponent ν for $d \geq d_c$. The third and fourth lines give the Flory formulae for ν and their expansions in $\varepsilon \equiv d_c - d$ to lowest order. The fifth line gives the RG expansions, emphasizing the lack of agreement between ν_F and ν_{RG} in the immediate vicinity of d_c. Note that for the gel, ν is usually denoted ρ; it gives the dependence of the mean cluster diameter on the number of monomers in the cluster. Finally, we give the corresponding values of D^+, the "fractal" dimension ([7.16] and references therein). We note that D^+ is the same for branched polymers and gels above d_c, even though the numerical values of d_c differ

	(a) linear polymer	(b)branched polymer	(c) gel
d_c	4	8	6
$\nu(d \geq d_c)$	1/2	1/4	1/4
$\nu_F(d \leq d_c)$	$3/(d + 2)$[a]	$5/[2(d + 2)]$[b]	$2/(d + 2)$[c]
$\nu_F(d \lesssim d_c)$	$\frac{1}{2}(1 + \frac{1}{6}\varepsilon)$	$\frac{1}{4}(1 + \frac{1}{10}\varepsilon)$	$\frac{1}{4}(1 + \frac{1}{8}\varepsilon)$
$\nu_{RG}(d \lesssim d_c)$	$\frac{1}{2}(1 + \frac{1}{8}\varepsilon)$[d]	$\frac{1}{4}(1 + \frac{1}{9}\varepsilon)$[e]	$\frac{1}{4}(1 + \frac{5}{42}\varepsilon)$[f]
$D^+(d \geq d_c)$	2	4	4
$D^+(d \lesssim d_c)$	$2(1 - \frac{1}{8}\varepsilon)$	$4(1 - \frac{1}{9}\varepsilon)$	$4(1 - \frac{5}{42}\varepsilon)$

[a][7.2], [b][7.8,9], [c][7.1], [d][7.5], [e][7.11], [f][7.17-19]

7.1.3 Gels

Let us return to our simple example, the reaction of f-functional monomers (Fig. 7.1c). Figure 7.2 illustrates a specific case, trimethoyl benzene, with f = 3.

1 Specifically, ν is decreased. The slower increase in the linear diameter of the polymer when branching is allowed may be understood physically by realizing that monomers which form branches often do not contribute to an increase in the linear diamter ξ. The more branches that form, the more the number of additional branches that *can* form on the next step. This "cascade effect" causes a change in the *exponent* as opposed to the *amplitude* in (7.1).

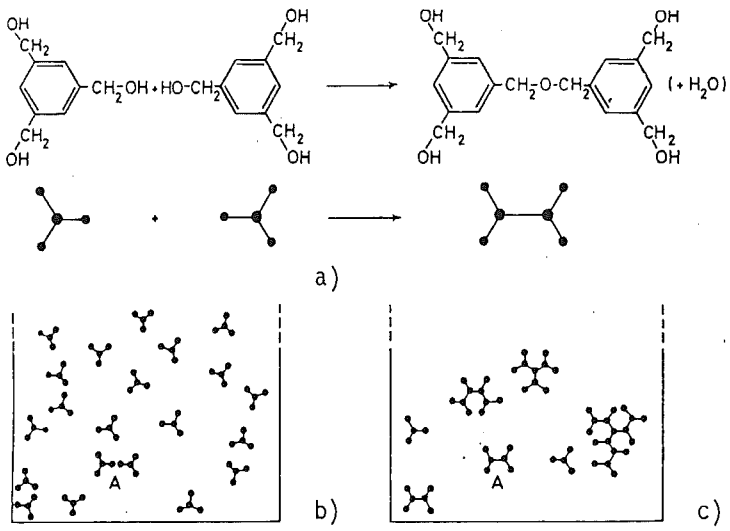

Fig.7.2a-c. Illustration of the simplest gelation phenomenon, polyfunctional condensation of f-functional monomers. The f-functional monomer shown in (a) is trimethoyl benzene; it has three "functional" groups that can react to form ether linkages. If f were two, then the most complex structures possible would be chains and rings; however, since f > 2 here, branched networks form. In (b) and (c) beakers are shown at successive stages of reaction. Adapted from [7.20]

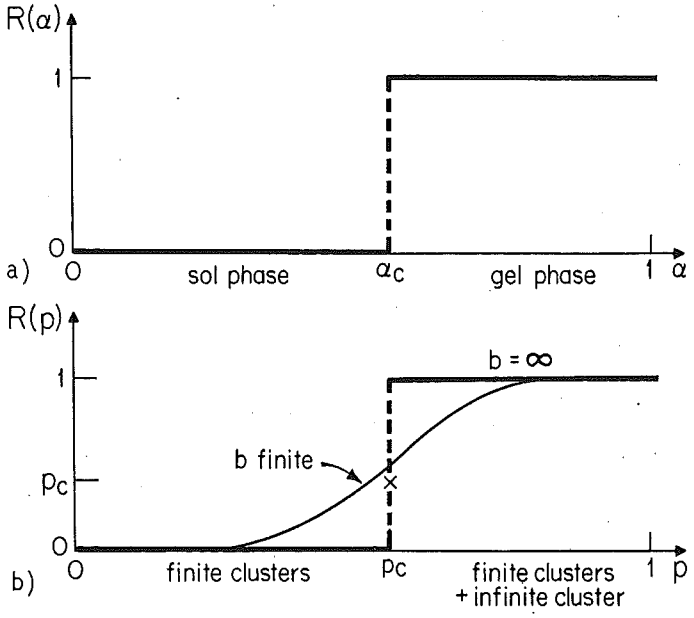

Fig.7.3a,b. Illustration of the analogy between (a) the gelation threshold and (b) the percolation threshold. In (a) the function $R(\alpha)$ denotes the probability that in an infinite system there is at least one molecule infinite in spatial extent. In (b), $R(p)$ denotes the probability that there is at least one cluster infinite in spatial extent. The step function is for an *infinite* lattice, while the curve denotes the same probability function for a *finite* lattice of edge b (for which "infinite cluster" is interpreted to mean "spanning cluster"). The rounding apparent for the finite system becomes successively less pronounced as the system grows in size. In the limit of an infinite system, $R(p_c)=p_c$, so that p_c is a fixed point and the system is scale invariant. Thus in the renormalization group approach, percolation phenomena naturally divide into three regimes ($p < p_c$, $p = p_c$, and $p > p_c$)

Each benzene ring has three reactive methyl groups; methyl groups from two different monomers can react to form an ether linkage [7.20]. The reaction is characterized by a parameter α, termed the *conversion*, which is the fraction of reacted methyl groups. If $\alpha = 0$, only monomers are present. If $\alpha > 0$, finite polymers can exist in all sizes. However the probability of forming an infinite polymer molecule is zero for all α less than a critical value α_c. For $\alpha > \alpha_c$ the probability for an infinite molecule to occur jumps from zero to unity. Thus the *connectivity* of the system changes drastically at $\alpha = \alpha_c$, and this "phase transition" is termed gelation (Fig.7.3a).

7.2 Three Mathematical Models

In the study of polymer statistics, it is often useful to treat lattice models in which there is a 1:1 correspondence between monomers and sites of a lattice. The f reactive end groups may be thought of as directed along the f lattice bonds emanating from each lattice site. It is widely believed that such models display the same critical behavior as continuum systems ([7.21,22] and references therein).

In this section, we shall formally define the three lattice statistical models that are relevant to the three polymeric systems discussed above. For pedagogical clarity, we begin with a simple model used to describe gelation–percolation on a Cayley tree pseudolattice [7.23-29].

7.2.1 Percolation

The first successful model to capture the essential physics of the gelation threshold was proposed 40 years ago by FLORY, and developed in a series of classic papers by both FLORY [7.23] and STOCKMAYER [7.24]. The Flory-Stockmayer (FS) model not only predicts the existence of a gelation threshold α_c, but also provides the "critical exponents" characterizing the behavior of various quantities such as the gel fraction, degree of polymerization, and mean end-to-end distance ξ.

The FS model was formulated in a fashion that at first sight seems to be lattice independent. One merely requires that a given polymer be forbidden to loop back upon itself, i.e., intramolecular interactions are excluded. Today we recognize this assumption as fully equivalent (as far as critical behavior is concerned) to the statement that the polyfunctional monomers be required to occupy the sites of a Cayley tree: to each polymer configuration formed from bonding of f-functional monomers, there is a one-to-one correspondence with a configuration of bonds on a Cayley tree whose coordination number is equal to f [7.25-28].

In reality, loops do form–both by inter- and by intra-molecular bonding. What is the effect of allowing for the loops? Clearly the threshold will increase, since the extra bonds necessary to create the loops do not contribute to the for-

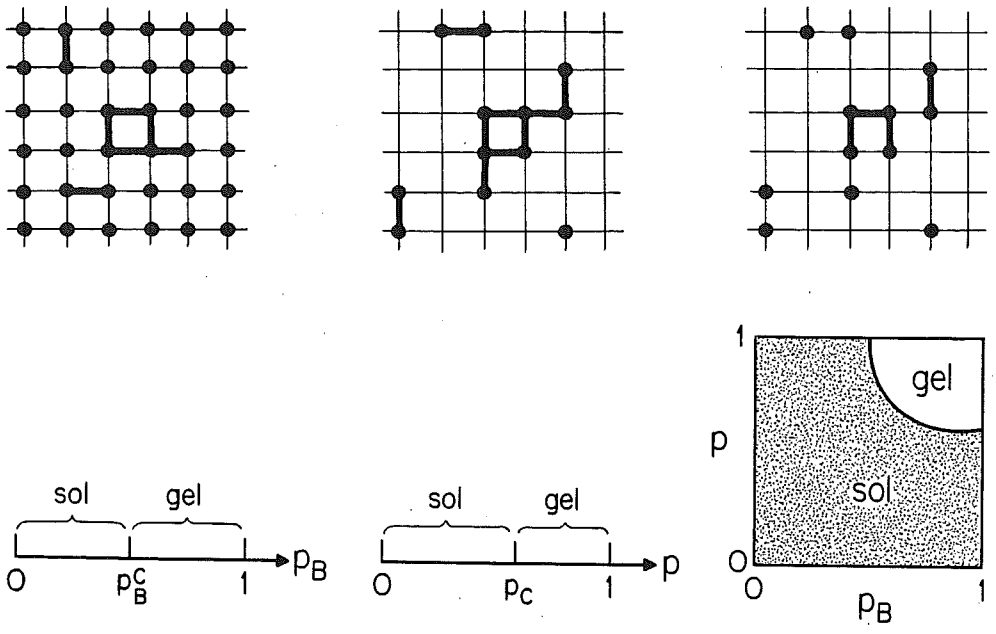

a) Bond percolation b) Site percolation c) Site-bond percolation

Fig.7.4a-c. Schematic illustration of (a) bond percolation, (b) site percolation, and (c) "site-bond" percolation, and their associated phase diagrams. The original Flory theory of polyfunctional condensation is an example of bond percolation, while many models of random magnets involve site percolation. Site-bond percolation is a hybrid model [7.31] that can be treated by position-space renormalization group methods [7.32,33]. When correlation is included among the sites, the resulting gelation model is capable of incorporating solvent effects and phase separation [7.34-39]

mation of an infinite branched network. Perhaps more significantly, the critical behavior of the system in the immediate vicinity of the gel point will be characterized by quite different exponents for $d < d_c$, where d_c denotes the upper marginal dimension. For gelation, d_c is believed to be six [7.30].

Thus let us consider a simple lattice model which describes polymers of arbitrary configuration, including polymers with loops. Suppose that all the sites of an infinite lattice of coordination number $z = f$ are occupied with monomers. Further, imagine that neighboring pairs of monomers can randomly form bonds, with probability p_B (Fig.7.4a). If p_B is small, the monomers group into small oligomers or "clusters". As p_B increases, the clusters grow larger; they also become more "ramified" or stringy ([7.30,40,41a]; the "ramified" incipient infinite character has been quantified in [7.41b,c]). As long as p_B is not too large, the clusters remain finite: e.g., if we pull on clusters at both "ends" of the lattice, there is no elastic restoring force. However, when p_B reaches a critical threshold, the bond network contains an infinite cluster which gives rise to a nonzero elastic modulus.

We have just described bond percolation, which may be thought of as a transcription of the Flory model of gelation from a Cayley tree pseudolattice ("no loops") to a real lattice (where loops are allowed). The analogous model of site percolation

is described as follows. Imagine that the sites of the same lattice are now *randomly* occupied with probability p by monomers, and that *all* possible bonds form between nearest-neighbor monomers.[2] One now considers the clusters of sites formed in this case (Fig.7.4b). Site percolation has also proved useful in describing a variety of phenomena occurring in other systems, e.g., dilute magnets.

The position-space renormalization group methods we develop here are equally applicable to both bond and site percolation. Here we shall mainly concern ourselves with site percolation, treating bond percolation as an "extension" where appropriate.

A hybrid model, site-bond percolation (Fig.7.4c), has been proposed and successfully applied to the description of gelation in a solvent ([7.31,34,35] and references therein). In site-bond percolation, sites are occupied by monomers with probability p and by solvent molecules with probability q = 1 - p. Bonds connecting neighboring pairs of monomers are intact with probability p_B, which in general is dependent upon external parameters such as temperature and pH. When correlation is permitted among the monomers and solvent molecules, the resulting "site-bond correlated percolation" model describes phase separation data obtained in the gelatin-ethanol-water system [7.36].

The models described above display singular behavior in their connectivity properties at their percolation thresholds. These phenomena are true phase transitions, and renormalization group methods have proved useful in their qualitative and even quantitative description. Of course, phase transitions can only occur in infinite systems. In a finite lattice with N sites, connectivity properties become "rounded" as indicated in Fig.7.3b. For example, let us consider the probability R(p) that a network has a nonzero elastic modulus. This will happen when a single cluster (polymer) spans the entire lattice. For N small, one can enumerate all configurations of the system, and thereby calculate this probability. Thus

$$R(p) = \sum_{\text{config}} P_{\text{config}} f_{\text{config}} , \tag{7.4}$$

where the summation is over all 2^N configurations of the system. Here $P_{\text{config}} = p^L q^{N-L}$ is the probability of a particular configuration of L occupied sites, while f_{config} is unity if that configuration "spans" and zero otherwise [7.42]. Our reason for focusing on R(p) is that it will serve as a recursion relation in the renormalization group approach, while f_{config} will be a "weight function". The connectivity implied by the existence of a spanning path is the physical criterion we will use to rescale probabilities.

---

2 Originally, site percolation was thought of as being a model in which all nearest-neighbor bonds are occupied, independent of the site occupancy. Of course, the connectivity properties of both models are the same.

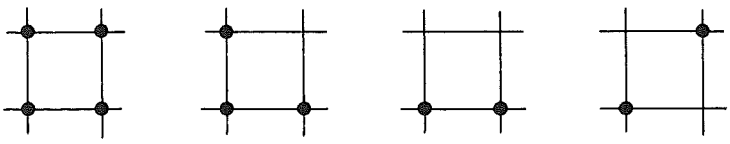

Fig.7.5a-d. Some of the 2^4 configurations that arise in the position-space renormalization group for site percolation on the square lattice using a b = 2 cell. Configurations (a-c) span from East to West, while configuration (d) does not

As an example of R(p), consider a finite lattice with only 4 sites. There are 2^4 configurations, some of which are shown in Fig.7.5. The reader can readily verify that if "spanning" is defined from East to West, then

$$R(p) = p^4 + 4p^3q + 2p^2q^2 \quad . \tag{7.5}$$

The function R(p) has been evaluated exactly for $N \leq 16$, and by Monte Carlo methods for N up to 250,000 [7.43,44]. As N increases, R(p) becomes sharper, and approaches the step function sketched in Fig.7.3 as $N \to \infty$.

7.2.2 Self-Avoiding Walks

Consider again the infinite square lattice, and choose a site at random to be called the origin. Consider now the set of all L-step random walks emanating from the origin, subject only to the global constraint that each walk not intersect itself. Because of the global constraint, such a random walk is in fact not at all random; it is customarily called a "self-avoiding walk," and given the acronym SAW [7.45,46].

We can ask many nontrivial questions about the statistical properties of SAWs. For example, let us define c_L to be the number of different self-avoiding walks of L links ("steps") that emanate from the origin; an L = 5 example is shown in Fig. 7.1a. Clearly $c_1 = 4$, since there are four different one-step walks, depending on whether the compass direction of the first step is N,E,S, or W. Similarly $c_2 = 12$ since each of the one-step walks can be continued in three different ways.[3]

Although enumerating the first few terms is easy, the enumeration of the coefficients c_L for arbitrary L is a combinatorial problem of classic difficulty. It is, however, of particular interest because the generating function, defined by

$$G(K) = 1 + \sum_{L=1}^{\infty} c_L K^L \quad , \tag{7.6}$$

3 For the square lattice the coefficients c_L have been enumerated by machine computation to order L = 24 by SYKES and collaborators [7.47].

displays a power-law singularity of the form

$$G(K) \sim |K - K_c|^{-\gamma} \quad . \tag{7.7}$$

We call the exponent γ, because in the $n \to 0$ limit of the n-vector model, G(K) is proportional to the susceptibility above the critical temperature [7.1,2,7]. The critical parameter K_c is usually denoted $1/\mu$, where $\mu = \lim_{L\to\infty} c_L/c_{L-1}$ is called the connective constant [7.47] because asymptotically, μ monomers can connect to an existing walk to form the next larger walk. For a random walk, $\mu = z$; for a SAW, $\mu \leq z - 1$.

7.2.3 Lattice Animals

In the models we have been considering, polymers can be thought of as clusters on a lattice. Such clusters are often called *lattice animals*, because they represent all the possible shapes that can be formed out of the constituent elements. Linear lattice animals that do not self-intersect (i.e., are loopless) are just the SAWs we discussed above. However, general lattice animals may branch and may form loops (Fig.7.6). Lattice animals having the same number of elements (sites or bonds) may be further distinguished by the number of perimeter sites and/or bonds.

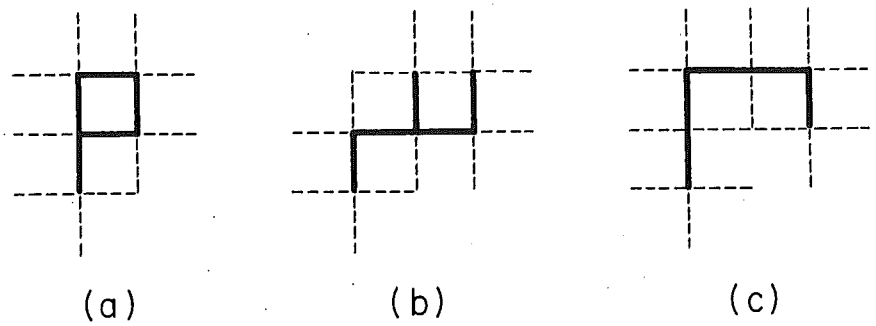

Fig.7.6a-c. A 5-bond branched lattice animal with looping is shown in (a), while (b) shows a 5-bond branched lattice animal without a loop. (c) shows a linear 5-bond lattice animal with neither branching nor loops, i.e., a SAW [the crossover between the lattice animal problem and the SAW problem is discussed in Sect.7.3.3]. In the *general* lattice animal problem, each of these lattice animals is weighted by a factor K^5q^t, where t is the number of perimeter bonds [cf. (7.33)]. The "pure" random animal problem obtains in the limit q = 1, for which all three configurations shown here are equally probable. If q = 1 - K, one obtains bond percolation [the crossover between pure random animals and bond percolation is also discussed in Sect.7.3.3]

In studying the structure of lattice animals, a particularly useful quantity is the probability P(L,p) that a randomly selected site or bond in the lattice is a member of an L-element cluster. In general, the functions P(L,p) are determined "recursively" from P(L - 1,p) by adding an element in all possible ways to each animal of size L - 1. For example, for *site* animals on the square lattice, the reader

can easily verify that[4] $P(1,p) = pq^4$, $P(2,p) = 4p^2q^6$, and $P(3,p) = 3p^3(4q^7 + 2q^8)$.

The general form of $P(L,p)$ is [7.30,52]

$$P(L,p) = Lp^L D(L,q) \quad , \tag{7.8a}$$

where the factor p^L arises from the L occupied sites (or bonds), and the "perimeter polynomial" $D(L,q) = \sum_t g_{Lt} q^t$ arises from the unoccupied "perimeter" that bounds the cluster. Here g_{Lt} is the number of lattice animals with perimeter t. Since $D(L,q)$ gives the number of distinct lattice animals of L elements, grouped according to the number of perimeter elements,

$$A_L \equiv D(L,q = 1) \tag{7.8b}$$

gives the total number of L-element lattice animals.

A generating function for lattice animals, analogous to that for SAWs, is given by

$$G(K) = 1 + \sum_{L \geq 1} A_L K^L \quad . \tag{7.9}$$

Note that (7.9) subsumes (7.6), for if we restrict ourselves to linear bond animals, the generating functions are the same.

Both the site and bond animal generating functions display a power-law singularity of the form[5]

$$G(K) \sim |K - K_c|^{\theta - 1} \quad . \tag{7.10}$$

The critical parameter K_c is usually denoted $1/\lambda$, where λ is called the "growth parameter" [7.48] because asymptotically $A_L/A_{L-1} \to \lambda$. Thus in an enumeration of the number of animals of size L, asymptotically one finds λ times as many animals as at the previous order (for a Cayley tree, $\lambda = z$).

---

4 The functions $P(L,p)$ for site animals have been evaluated exactly on the square lattice for $L \leq 19$ [7.48], and on the general-d hypercubic lattice for $L \leq 8$ [7.49]. For $2 \leq d \leq 7$, $P(L,p)$ has been evaluated for certain values of p by Monte Carlo methods for L up to about 10^6 [7.50,51].

5 Exact results exist for a one-dimensional lattice [7.53], for which $G(K)=(1-K)^{-1}$. Thus $\lambda = 1$ and $\theta - 1 = -1$. The A_L can also be evaluated exactly for the Bethe lattice [7.25], giving the result $\theta - 1 = 3/2$. It is believed [7.8-12,49] that θ takes on the value 5/2 for all systems with $d > 8$. For $1 < d < 8$, the A_L have been evaluated exactly for small values of L [7.48,49,54,55]; one finds that θ varies smoothly with d. PARISI and SOURLAS [7.10] have recently argued that $\theta(d) - 1 = \sigma(d') + 1$. Here, $\sigma(d') + 1$ is the exponent characterizing the singularity in the complex H plane [7.56] of the Gibbs potential $G(H,T_0)$ for an Ising model of dimensionality $d' = d - 2$ at a fixed temperature $T_0 > T_c$.

7.3 Position-Space Renormalization Group Treatment

In order to apply position-space renormalization group approaches to polymer models, one must first establish a connection between the sorts of "geometric phase transitions" exhibited by polymer systems and the more conventional kinds of phase transitions familiar from extensive studies of thermal critical phenomena. To this end, an important development was the observation of de GENNES [7.5] that the limit in which the number of monomers in a linear polymer tends to infinity, corresponds to the temperature of a magnetic system approaching its critical value T_c.

Polymer systems also resemble thermal systems in that both have the characteristic of self-similarity near their respective critical points. As one approaches the critical point of a magnet, fluctuations occur on larger and larger length scales until at the critical point there is no longer a "maximum" characteristic length. Viewed from a large length scale, the system is self-similar, or scale invariant. Similarly, for a polymer system at the "critical fugacity", polymers of all sizes occur, and this system is also scale invariant. At this point the polymeric system undergoes a phase transition from a state of *local* connectedness to one of *global* connectedness.

7.3.1 Percolation

a) *Basic Approach*

For the sake of clarity, we shall first discuss the position-space renormalization group treatment of percolation. It is widely appreciated that the $Q \to 1$ limit of the Q-state Potts model [7.57] corresponds to pure bond percolation [7.58]. This fact provided the initial bridge between conventional "thermal" critical phenomena and the sort of "geometrical" critical phenomena exemplified by percolation. In particular, the Potts Hamiltonian has been treated by both momentum-space renormalization group [7.17-19,59] and by position-space renormalization group [7.17,60,61], yielding predictions for percolation quantities in the limit $Q \to 1$.

A Hamiltonian, however, is not necessary for studying percolation. Indeed, in the "pure" percolation problem, the elements (sites or bonds on a lattice) are placed entirely at random with no interactions between them. However, singularities nevertheless occur in the geometric properties of the physical clusters.

In fact, the mere existence of a diverging length scale is sufficient to motivate the use of the renormalization group. STINCHCOMBE and collaborators [7.62-64] showed how a decimation procedure applied directly on the bond occupation probabilities — in which a set of vertices is summed over, leading to renormalized bond probabilities on a rescaled lattice — is equivalent to summing out degrees of freedom in the Potts partition function. Another approach for the bond problem, also treating the probabilities directly, was followed by KIRKPATRICK [7.65], who used the MIGDAL-KADANOFF approach [7.66].

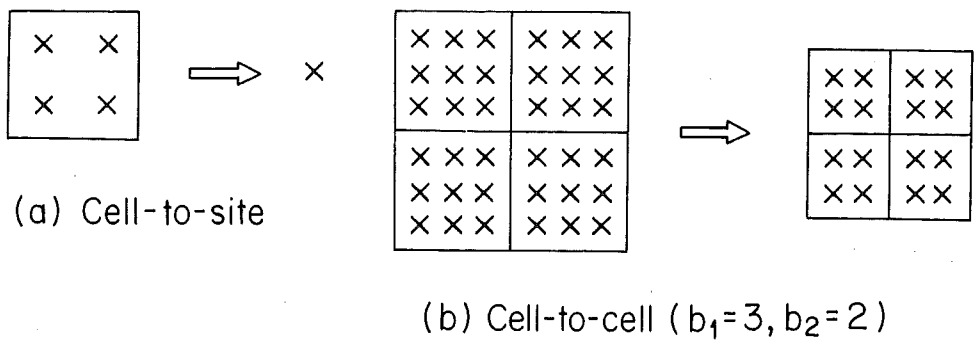

Fig.7.7a,b. Comparison between (a) the conventional "cell-to-site" construction with b=2, and (b) a "cell-to-cell" construction with $b_1=3$, $b_2=2$. By covering the lattice in two different ways, first with cells of side b_1 and then with cells of side b_2, we obtain a cell-to-cell transformation with rescaling length b_1/b_2

The numerical predictions based on the early renormalization group work were less accurate than those obtained from extrapolation of series expansions. One reason for this initial inaccuracy is related to the fact that the approaches all basically involved uncontrolled approximations.

As a simple - but readily improvable - position-space renormalization group, let us now consider a cell approach [7.42]. Partition a square lattice into cells of edge b, each containing b^2 sites; an example for b = 2 is shown in Fig.7.7a. After a renormalization transformation these cells play the role of "renormalized" sites. If the sites are occupied with probability p, then the cells may be defined to be occupied with probability p', where

$$p' = R(p) \quad . \tag{7.11}$$

The function R(p) was defined in (7.4) for an arbitrary cell and illustrated in (7.5) for the case b = 2. It is simply the probability of there being a path that spans the cell from East to West. If such a spanning path exists, then, according to this choice of weight function, the cell is occupied. Equation (7.11) serves as a simple, albeit highly approximate, position-space renormalization group transformation. The fixed points p^* of the transformation (7.11), which satisfy the relation

$$p^* = R(p^*) \quad , \tag{7.12}$$

include two trivial fixed points at $p^* = 0, 1$ and also a critical fixed point at a value that depends upon b. In this one-parameter position-space renormalization group, the critical fixed point gives an estimate for the value of the nonuniversal quantity p_c. For the b = 2 example of (7.5), $p^* = 0.62$, which should be compared with more accurate estimates, $p_c = 0.59$ ([7.67] and references therein).

To calculate the critical exponent ν_p from this simple transformation, we note that all lengths in the rescaled system have been reduced by a factor of b from the lengths in the original system.[6] Hence the connectedness length ξ transforms as

Footnote 6 see next page

$\xi' = b^{-1}\xi$. Since $\xi \sim |p - p_c|^{-\nu_p}$ and p_c corresponds to p^*, we obtain

$$|p' - p^*|^{-\nu_p} = b^{-1}|p - p^*|^{-\nu_p} \quad . \tag{7.13}$$

On the other hand, we can subtract (7.12) from (7.11). Because the transformation $R(p)$ is analytic near p^*,

$$p' - p^* = R(p) - R(p^*) = \lambda(p - p^*) \quad , \tag{7.14}$$

where $\lambda = dR/dp|_{p^*}$. If (7.14) and (7.13) are to be consistent, we must have $\lambda^{-\nu_p} = b^{-1}$ or

$$\nu_p = \ln b/\ln\lambda \quad . \tag{7.15}$$

For the $b = 2$ example in question, we find $\nu_p \simeq 1.6$, which should be compared with the possibly exact value $\nu_p = 4/3$ [7.68-70].

This completes our simple position-space renormalization group example for the case $b = 2$. The results for p_c and ν_p are not expected to be very accurate, due to the "one-shot" nature and the simplicity of the approximation. It is, however, useful to try to understand the source of this error; in so doing, a natural method for compensating for the error will arise. Figure 7.8 shows a possible occupancy configuration for four adjacent cells. Notice that cells B and C are connected in the original problem, but not in the rescaled problem. Conversely, cells A and D are not connected in the original problem, but are connected in the rescaled picture. Thus with the simple connectivity rule, the rescaled cell problem may not faithfully mirror the connectivity of the original problem.

In the conventional renormalization group approach, intercell connections can be "patched up" by introducing additional couplings (further neighbor, multisite, etc.). The entire set of couplings must then be renormalized. This leads to the usual ideas about relevant and irrelevant operators, and flow trajectories. This method is most useful when there is a crossover effect to study (see Sect.7.3.3). In pure percolation, all the additional couplings are irrelevant, and their main effect is to complicate the calculation. The number of parameters grows quickly,

---

6 The connectedness length ξ_p characterizes the exponential decay with r (near but not at p_c) of the pair connectedness function $C(r)$, which in turn gives the probability that a site at position r is occupied and connected to a site at the origin. The singularity in ξ_p at the "percolation critical point" ($p=p_c$, $L=\infty$) and its behavior near the critical point is described by the exponent ν_p if the variable $p-p_c$ is used, and by the exponent ν if the variable L is used. The exponents ν_p and ν are related by $\nu_p = \nu\Delta$, where Δ is the "gap exponent," and $\Delta = \beta\delta = \beta + \gamma$ by scaling. For largely historical reasons, the exponent ν is denoted ρ in much of the percolation literature, while the exponent ν_p is denoted ν.

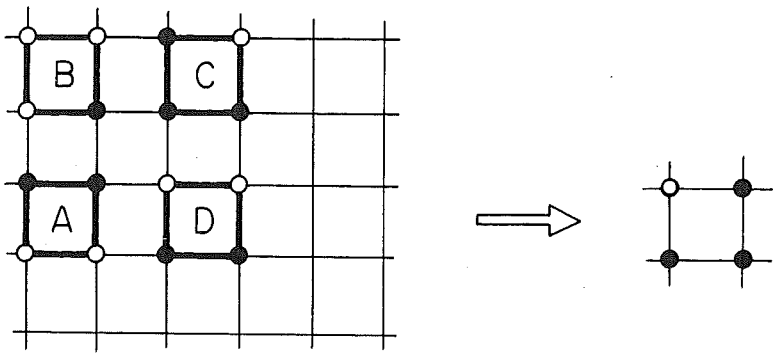

Fig.7.8. Rescaling a lattice by forming cells out of groups of sites. Four-site cells on the square lattice are shown, with dots representing occupied sites. In this example, cells C and D are both "occupied" (each cell can be traversed), and therefore connected on the *cell* level. On the *site* level, however, we cannot connect them. On the other hand, cells A,B, and C are connected on the *site* level, though only the next-neighbor cells, A and C, are occupied. These incorrect connections force one to either introduce nearest-neighbor, further-neighbor, and multisite probabilities, or to go to larger cells where the "interfacing" error plays a smaller relative role [7.42]

but there is no guarantee that there will be a corresponding return in increased accuracy. To bypass these complications, we next consider a different approach in which only one parameter, p, is kept.

b) Extensions

1) Large-Cell Monte Carlo Renormalization Group. In order to improve upon the one-parameter, "small-cell" method, we note that the error introduced by incorrect intercell connections is essentially a surface effect; as such, it should get smaller as the cell size gets bigger [7.71]. This in fact happens. Thus our approach here will be to retain the single-parameter position-space renormalization group, but increase b systematically. For b = 3, the summation in (7.4) extends over $2^9 = 512$ configurations, while for b = 4 and 5, there are 2^{16} and 2^{25} configurations respectively. Although 2^{25} is a rather large number, one may use a computer to determine f_{config} for each of these configurations, and thereby obtain R(p) exactly. The values of $p^*(b)$ and $\nu_p(b)$ become increasingly accurate with larger b, but the convergence in b is rather slow. Nevertheless, we can estimate the critical parameters fairly accurately, based on the largest values of b (b = 5) for which R(p) may be computed in closed form.

However, we can do better still! The systematic improvement of the small cell results with b suggests that we *extrapolate* our finite-b results to $b \to \infty$, somewhat in the spirit of extrapolations based on exact enumeration methods. The renormalization group extrapolation procedure parallels the phenomenological theory of finite-size scaling([7.72]; see also the recent justification of finite-size scaling in [7.73]). In this sense, the errors in these extrapolated estimates are

less "uncontrolled" than those made on the basis of other renormalization group methods of successive approximations—such as higher order cumulant expansions—for which there is no systematic procedure for extrapolating successive estimates for the critical parameters.

For example, to extrapolate the successive estimates of $p_c(b)$, finite-size scaling considerations [7.43,44] suggest

$$|p^*(b) - p_c| \sim b^{-1/\nu_p} \quad . \tag{7.16a}$$

Furthermore, from considerations of the error in the position-space renormalization group eigenvalue, a likely form for $\nu_p(b)$ is [7.43,44,74]

$$|\nu_p(b) - \nu_p| \sim A_1(\ln b)^{-1} + A_2(\ln b)^{-2} \quad . \tag{7.16b}$$

Thus the error will decrease as b increases in a *predictable* fashion, and a sequence of values of $p^*(b)$ and $\nu_p(b)$ can be used to extrapolate the limiting $(b \to \infty)$ behavior.

However, for accuracy comparable to series, one must extrapolate using values of $p^*(b)$ and $\nu_p(b)$ for $b > 5$. To do this, a large-cell Monte Carlo renormalization group was developed [7.43,44]. This method shows the close connection of one-parameter position-space renormalization groups with finite-size scaling. The large-cell calculations and extrapolations for site percolation have been carried out for the square lattice [7.43,44], and for the triangular lattice [7.74], using an algorithm based on the work of HOSHEN and KOPELMAN [7.75]. This algorithm tests which realizations span, and hence have $f_{config} = 1$. One finds [7.44] that R(p) can be calculated with remarkable accuracy by sampling comparatively few of the 2^N $(N = b^2)$ of the possible configurations.[7]

The results of the square lattice calculations are summarized in Fig.7.9a [which is based on (7.16a)], and in Fig.7.9b [which is based on (7.16b)]. Actually, two sets of curves are shown in Fig.7.9a. The set labelled R_1 corresponds to the connectivity weight function described earlier, which assigns the value $f_{config} = 1$ if the configuration spans the cell in the East-West direction. The set labelled R_0 differs in that $f_{config} = 1$ if the configuration spans *either* in the East-West *or* in the North-South direction. Notice that even for the largest cell size considered, the estimates $p^*(b)$ and $\nu_p(b)$—though accurate by usual position-space renormalization group standards—are still not as accurate as one would desire; in fact, they are only beginning to approach the accuracy available from series expansions [7.30,52]. However, since the dependence of $p^*(b)$ and $\nu_p(b)$ follows

---

7 For example, for b = 500, N = 250,000; there are roughly $10^{75,000}$ configurations! The function R(p) was calculated by averaging the results of only 10^3 total realizations. The sharpness of R(p) for a system with this many sites made it highly probable that when R(p) was calculated again, using 10^3 *different* realizations, the two calculations agreed to remarkable accuracy.

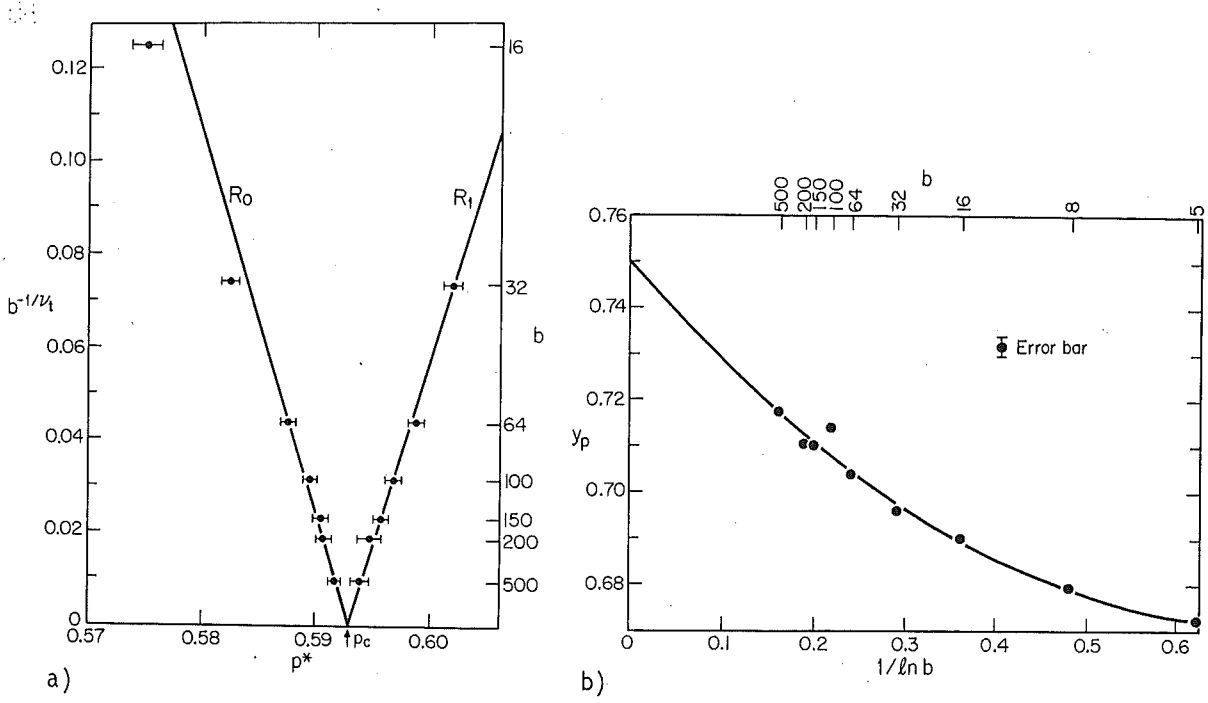

Fig.7.9. (a) Extrapolation of the sequence of fixed points $p^*(b)$ obtained from connectivity rules R_0 and R_1 using (7.16a). We have chosen the trial value of $\nu_t = 4/3$, for this plot. Both curves approach approximately the same final estimate of p_c as $b \to \infty$. (b) Quadratic extrapolation against $1/\ln b$ for y_p, using rule R_0 and (7.16b). The error bar shown is representative. The solid curve is the least-squares fit, $y_p(b) = 0.7490 - 0.0221/(\ln b) + 0.0157/(\ln b)^2$

(7.16), the finite-b results can be extrapolated to the limit $b \to \infty$. We see from Figs.7.9a,b that the $b \to \infty$ extrapolation provides estimates for p^* and ν_p that differ substantially from any of the finite-b values. These *extrapolated* estimates are as accurate as series estimates, and are possibly even somewhat more accurate. One obtains $p_c = 0.5931 \pm 0.006$ and $\nu_p = 1.33 \pm 0.01$, the latter result requiring that we keep quadratic terms in (7.16b)[8]. Moreover, the fact that the estimates derived from "connectivity rule R_0" agree with those obtained from "connectivity rule R_1" adds further confidence to the results obtained. The result for ν_p agrees well with the widely accepted den NIJS conjecture [7.68].

2) Ghost Field. The above procedure gives the scaling power $y_p = \nu_p^{-1}$ analogous to the thermal scaling power in magnetic critical phenomena. To obtain all the percolation exponents, one must also calculate the scaling power y_h, which is analogous to the magnetic-field scaling power.

In percolation, the role of a magnetic field may be played by a ghost field ([7.53] and references therein). This can be defined in a variety of fashions

8 Quadratic terms were omitted in [7.44], and linear extrapolation resulted in the higher estimate $\nu_p = 1.354 \pm 0.015$. Quadratic terms are included in [7.74] and in Fig.7.9b, thereby reducing the estimate for ν_p.

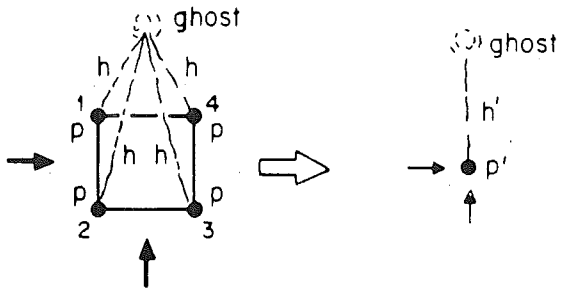

Fig.7.10. Illustration of the rescaling of a b=2 cell for site percolation on the square lattice in the presence of a nonzero "ghost field" h. The four original sites, each occupied with probability p, are transformed into a single renormalized site occupied with probability p'. The ghost bonds, which join to every site, are transformed into a bond with probability h' [7.43]

(see, e.g., the discussion in [7.52]). The simplest, conceptually, is to imagine that there is an extra "ghost site", exterior to the lattice, which is connected to every site in the lattice by a "ghost bond" which is occupied with probability h.

Equation (7.4) still determines R(p), except now f_{config} depends upon h. For example, consider the simple b = 2 case. For the configurations shown in Figs. 7.5a-c, $f_{config} = 1$ regardless of h. However, for the configuration shown in Fig. 7.5d, $f_{config} = h^2$, since if the two ghost bonds connected to the two occupied sites are both intact, then the configuration spans through the ghost site. Thus

$$p' = R(p,h) = R(p,h = 0) + 2p^2q^2h^2 \quad , \tag{7.17}$$

where R(p,h = 0) is given by (7.5).

It is also necessary to obtain a recursion relation for the ghost field h'. To determine this, notice that the presence of the ghost bonds allows the possibility of connecting to the ghost. This suggests that we can renormalize h by calculating the rescaled probability of being connected to the ghost. This connectivity is most appropriately expressed in terms of the probability of entering the cell *and* reaching the ghost, given by p'h' (Fig.7.10). This can be written in an obvious generalization of (7.4) as

$$p'h' = \sum_{config} P_{config} f_{config} \quad , \tag{7.18a}$$

where now the summation is over all 2^{2b^2} configurations of the b^2 sites and b^2 ghost bonds. For the case b = 2 shown in Fig.7.10, one finds [7.44]

$$p'h' = p^4Q_4 + 4p^3qQ_3 + p^2q^2(h + 5Q_2) + 3pq^3h \quad , \tag{7.18b}$$

where $Q_j \equiv 1 - (1 - h)^j$ is the probability that at least one of the j ghost bonds connecting the ghost to a set of j sites is intact. The recursion relation (7.18b) is derived by enumerating all connected paths from 2 adjacent edges of the cell to the ghost and calculating the sum of the probabilities for each such path (see Figs.7.5,10).[9] (Footnote 9 see next page).

By implementing this general procedure, and by using large-cell Monte Carlo methods for cells of size up to N = 250,000 sites, one can make a reliable extrapolation for y_h [7.44]. The result,

$$y_h = 1.898 \pm 0.003 \quad , \tag{7.19a}$$

is in remarkably good agreement with the closed-form extended den Nijs conjecture [7.76,77],

$$y_h = 91/48 = 1.896 \quad . \tag{7.19b}$$

3) Cell-to-Cell Transformation. Until now, we have considered the conventional position-space renormalization group approach of transforming from a system of cells to a new system of sites. This "cell-to-site" transformation is illustrated schematically in Fig.7.7a. However, one can also consider a transformation in which one passes from a system of cells of edge b_1 to a system of cells of edge b_2 [7.43] (Fig.7.7b). Such an implicit "cell-to-cell" transformation enables one to have a rescaling length b_1/b_2 which may be made close to unity.

We will illustrate the cell-to-cell transformation for the case of zero ghost field. There is then only one parameter, the occupation probability p. To calculate the critical exponent ν_p, we define $p_j = R(b_j;p)$ to be the renormalized occupation probability for a cell of size b_j ($j = 1,2$). Then the connectedness lengths of the two systems are related by

$$\xi(p_2) = (b_1/b_2)^{-1}\xi(p_1) \quad . \tag{7.20}$$

Hence the equation analogous to (7.13) is

$$|p_2 - p^*|^{-\nu_p} = (b_1/b_2)^{-1} \, |p_1 - p^*|^{-\nu_p} \quad , \tag{7.21}$$

where p^* is the fixed point of the cell-to-cell transformation. Note that (7.21) reduces to (7.13) if $b_2 = 1$ (and hence $p_1 = p$). The analog of (7.14) is

$$p_j - p^* = R(b_j;p) - R(b_j;p^*) = \lambda_j[p - p^*] \quad , \tag{7.22}$$

where $\lambda_j = [dR(b_j;p)/dp]_{p^*}$. Substituting (7.22) into (7.21), one obtains $(\lambda_2/\lambda_1)^{-\nu_p} = (b_1/b_2)^{-1}$, or

$$\nu_p = \ln(b_1/b_2)/\ln(\lambda_1/\lambda_2) \quad . \tag{7.23}$$

---

9 The first term is the product of the probability that all 4 sites are occupied, and that at least *one* of the 4 bonds connecting these four sites to the ghost site is intact. The second term is the probability that any 3 of the sites are occupied, and that at least one of the 3 bonds connecting these 3 occupied sites to the ghost site is intact. The third term is more complicated, since not all 6 of the configurations of two occupied sites are equivalent. If sites 2 and 4 in Fig.7.10 are occupied (as in Fig.7.5d), then the probability of being able to "get to the ghost" is simply p^2q^2h, since the ghost bond on site 2 must be intact, while the state of the ghost bond on site 4 is irrelevant. For the remaining 5 configurations of two occupied sites, the probability is $p^2q^2Q_2$, since either of the two ghost bonds must be intact. Finally, of the four configurations with only one occupied site, three of these will connect to the ghost, provided the corresponding ghost bond is intact. Each of these occurs with probability pq^3h.

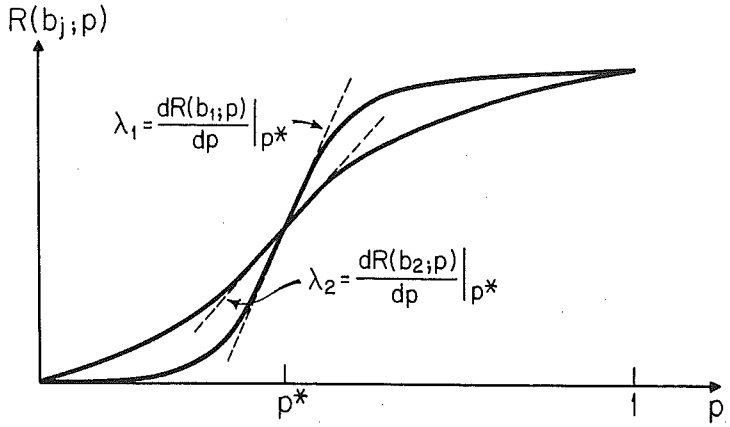

Fig.7.11. The dependence on p of the two renormalization group transformations $p_1=R(b_1;p)$ and $p_2=R(b_2;p)$. The fixed point of the transformation from p_1 to p_2 occurs where the two curves intersect. The exponent ν_p is obtained from the ratios of the slopes of these functions at the point of intersection using (7.23)

Again, (7.23) reduces to (7.15) if $b_2 = 1$ since then $\lambda_2 = 1$.

The location of the fixed point p^* and the calculation of the exponent ν_p is indicated geometrically in Fig.7.11. The cell-to-cell transformation has been used [7.43] to calculate $p^*(b_1,b_2)$ and $\nu(b_1,b_2)$ for all values of b_1,b_2 such that $b_2 < b_1 \leq 5$. It is found that the estimates are considerably better than for the corresponding cell-to-site transformations. Thus the strength of the cell-to-cell method is that it provides higher accuracy for a given amount of calculation—on the order of a cell-to-site calculation with b about 100. This higher accuracy probably results from the cancellation of similar errors in the functions $R(b_1,p)$ and $R(b_2,p)$. Additionally, extrapolation of the cell-to-cell scaling powers appears to converge as 1/b rather than 1/ln b.

For $b_1 > 5$, the transformations $R(b_j;p)$ are not known exactly. The combined approximations obtained from Monte Carlo simulations of two cell-to-site transformations give considerably larger error bars for the cell-to-cell transformation than for the corresponding cell-to-site transformation. This is apparent from Fig. 7.11 and the form of (7.23). A cell-to-cell Monte Carlo renormalization group that avoids this problem is also possible, but at present the cell-to-cell method is most useful when one has closed-form expressions for $R(b_j;p)$. For a discussion of a cell-to-cell approach in the context of thermal phase transitions, see Chap.3

4) Bond Percolation. For bond percolation, it is not immediately obvious how to choose a cell that covers the lattice with bonds, and rescales to another bond. One very useful choice is the family of cells [7.42] illustrated schematically for b = 2 in Fig.7.12. A simple weight function can be defined such that if the cell can be traversed horizontally, then the renormalized horizontal bond is considered to be intact, while if the cell can be traversed vertically, then the renormalized vertical bond is intact. The resulting recursion relation for b = 2, which is analogous to (7.5), is then

$$R(p) = p^5 + 5p^4q + 8p^3q^2 + 2p^2q^3 \quad . \tag{7.24}$$

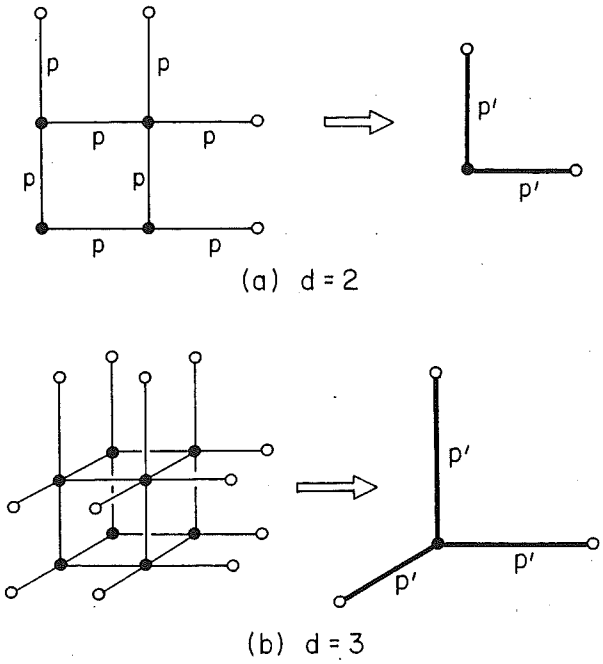

Fig.7.12a,b. The simplest b=2 cells for bond percolation for (a) the square lattice, and (b) the simple cubic lattice. The rescaled bonds are indicated by heavy lines and occur with probability p'

The nontrivial fixed point of the transformation $p' = R(p)$ is at $p^* = 0.5$, which agrees with the exact result, $p_c = 1/2$, for bond percolation on the square lattice. In fact, BERNASCONI [7.78] showed that this family of cells has the same self-duality as the square lattice itself, and thus $p^* = 1/2$ for all b. Unfortunately, the self-duality does not guarantee anything for the exponent. The above b = 2 recursion relation results in the reasonable approximation $\nu_p = 1.43$. KIRKPATRICK [7.79] has performed large-cell calculations for R(p) by Monte Carlo methods, with b = 16, 64, 200, and 512. However, he used a slightly different cell that does not preserve self-duality. Thus his sequence $p^*(b)$ is not fixed at 1/2, but only approaches 1/2 as $b \to \infty$. From his sequence $\nu_p(b)$, he estimates $\nu_p = 1.365 \pm 0.015$, which is just outside the now favored result $\nu_p = 4/3$. More recently, LOBB and KARASEK [7.80] calculated the sequence $\nu_p(b)$ using the self-dual cells and using many more cell sizes, to obtain an extrapolated values $\nu_p = 1.333 \pm 0.009$. Also their result, $y_h = 1.900 \pm 0.017$ for d = 2 bond percolation, agrees with the result in (7.19a) for site percolation. Also, MAGALHÃES et al. [7.81] and HEERMANN and STAUFFER [7.82] used this approach on the square bond problem, with good results.

5) Three Dimensions. Bond percolation calculations on the simple cubic lattice have been carried out analytically for b = 2 ([7.42]; see also [7.83] and references therein), using the cell shown in Fig.7.12b. KIRKPATRICK [7.79] extended this work to large cells and extrapolated to obtain $\nu_p = 0.845 \pm 0.015$. More recent calculations give $\nu_p = 0.88 \pm 0.01$ [7.82]. These position-space renormalization group numbers may be compared with the estimate $\nu = 0.83$ from series enumeration methods [7.84].

6) Other Percolation Properties

We have thus far restricted our discussion to the application of position-space renormalization group methods to the derivation of the percolation threshold and the two scaling powers y_p and y_h. The methods we have been describing may also be used to obtain other percolation quantities. Thus, e.g., one can calculate the exponent that describes the fashion in which the electrical conductivity of a percolation network approaches zero as $p \to p_c$ from above; the accuracy obtained in two dimensions [7.78,85-88] is comparable to that from series expansions [7.89].

In part because of its importance in understanding the physical phenomena occurring in electrical conductivity, the "backbone" of a bond percolation cluster has received considerable attention. SHLIFER et al. [7.90] have used large-cell Monte Carlo position-space renormalization group to calculate the scaling powers y_p and y_h for the backbone; their estimates agree quite well with independent Monte Carlo computer simulations [7.91,92].

VICSEK and KERTÉSZ [7.21] used large-cell methods to describe the connectivity properties of a continuum two-dimensional random system consisting of overlapping discs; their results are in general accord with Monte Carlo and series calculations [7.22], and support the notion that continuum systems – such as polymer gels – are in the same universality class as lattice systems.

KINZEL [7.93] has used the position-space renormalization group approach to calculate the cluster-size distribution function P(L,p), which is of particular interest because it obeys a scaling relation, the "cluster-number scaling hypothesis" [7.30].

7.3.2 Self-Avoiding Walks

a) *Basic Approach*

We begin by recalling the generating function G(K) defined in (7.6) for c_L, the total number of SAWs of L steps. As discussed above, G(K) for the SAW problem is singular at $K = K_c$, thus signalling the presence of a phase transition.

To formulate a position-space renormalization group for SAWs, one may follow the same general procedure used above to construct the position-space renormalization group for bond percolation. In percolation, the connectivity transition is signalled by the formation of an "incipient" infinite cluster [7.41,92,94]. This is a "critical" object which occupies a zero fraction of an infinite lattice, but which is globally connected. The weight function in percolation is chosen to detect this global connectivity. That is, cells with connected paths of bonds spanning the cell are mapped into renormalized bonds. Similarly, for SAWs we begin by recognizing that the critical object at the SAW threshold is a walk that is infinite in length. Moreover, this walk also occupies a zero fraction of an infinite system. Evidently the incipient infinite SAW plays the same role as the incipient infinite cluster in percolation. Accordingly, we might imagine that a "connectivity

rule" weight function analogous to the one used in bond percolation should also be applicable to the SAW problem. In such an approach, a renormalized bond is present if there is a connected, self-avoiding, path that spans a cell. This defines one possible weight function. The sum of the statistical weights for spanning SAWs has the form of a generating function, which is restricted due to the weight function. It is given by [7.95]

$$G(K) = \sum_{\text{config}} K^{L} f_{\text{config}} \quad . \tag{7.25a}$$

Here the summation is over all 2^B configurations of the B cell bonds. The function f is the weight function: f = 1 if the configuration represents a spanning SAW, and f = 0 otherwise. Different weight functions will differ in the definition of "spanning". To obtain a recursion relation, we equate this to the generating function on the cell level, where G'(K') = K'.

Let us consider, for example, the "corner rule" weight function [7.96-98] on the square lattice. The starting point of the SAW is fixed to be a corner of the cell, e.g., the lower-left corner, as shown in Fig.7.13 for b = 2. Walks that leave the cell by way of the right edge rescale to a single horizontal step, while walks leaving by the top edge rescale to a single vertical step. By symmetry, it suffices to consider only the 4 walks that rescale to a vertical step, and these are shown in Fig.7.13b. Weighting each walk with a factor of the monomer fugacity K for each of its bonds, one finds the recursion relation

$$K' = K^4 + 2K^3 + K^2 \quad . \tag{7.25b}$$

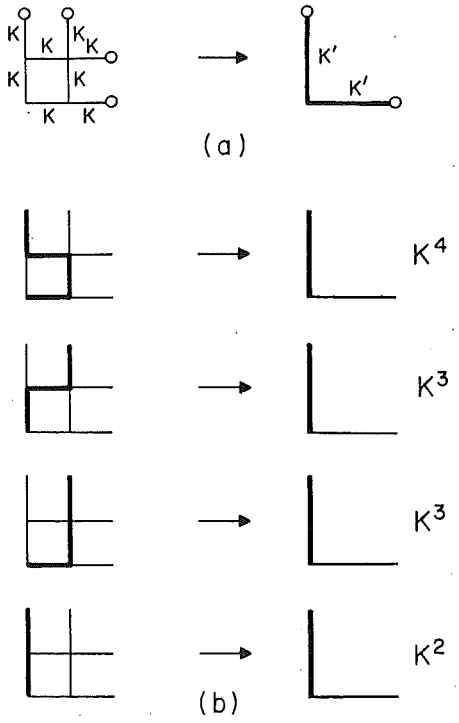

Fig.7.13. (a) The simplest b = 2 cell for the SAW problem on a square lattice (cf. Fig. 7.12a). (b) The four SAW configurations that contribute to a rescaled vertical step, which has fugacity K'

The structure of (7.25b) is analogous to the structure of the recursion relation (7.24) for bond percolation. We see that there exist 3 fixed points, two trivial ones at $K^* = 0, \infty$, and a critical one at a finite value of K, whose location is dependent on the details of the approximation. We interpret them as follows:

1) There is an "empty lattice" fixed point $K^* = 0$; the recursion relation (7.25b) faithfully rescales K = 0 into another empty lattice with K' = 0. For all $K < K^*$, SAWs are finite in length, and they shrink upon each rescaling. The limit of this process is a polymer of size zero, as described by the $K^* = 0$ fixed point.

2) There is a "full lattice" fixed point at $K^* = \infty$. In bond percolation, the full lattice has every bond intact, while in the SAW problem, every *site* of the lattice is visited, and the SAW densely packs the lattice.

3) There is a critical fixed point at $K^* = 0.466$ (for the corner rule) corresponding to the critical fugacity $K_c = 1/\mu$; the best estimate from exact enumeration procedures is $K_c = 1/\mu = 0.379003 \pm 0.000015$ [7.47]. Moreover the divergence of ξ as $K \to K^*$ is given by $\nu = \ln b/\ln\lambda = 0.715$, where λ is the slope of K'(K) at K^*; this should be compared with numerical estimates for ν in two dimensions in the range 0.74-0.75 [7.1].

There are several types of approximation in this renormalization procedure. For example, there is the restriction placed on the SAW that its starting point be fixed at the corner of the cell. This is an approximation since it is unlikely that a traversing SAW in one cell will terminate at the starting point for an SAW in the next cell. Also, there exist configurations that can contribute to an infinite SAW that do not span the cell at all, e.g., a walk that leaves the cell by the same edge at which it enters. To avoid these sorts of problems, one possibility is to choose a better weight function. For example, one can in principle average over all possible starting points of a walk in the cell. However, because the starting points are not equivalent, a weight function formally akin to the transfer matrix has proven more useful. The best results seem to be obtained if one uses periodic boundary conditions, which correspond to wrapping the cell onto a cylinder or torus [7.98,99]. A toroidal cell is translationally invariant, and all starting points are equivalent. The weight function then counts all walks that wind around the torus once with respect to the origin. Thus for the simple case b = 2, one has [7.98]

$$K' = 2K^4 + 4K^3 + K^2 \quad . \tag{7.26}$$

The nontrivial fixed point $p^* = 0.366$ and the estimate $\nu = 0.690$ are both reasonable for such a small cell, though ν is worse than by the corner rule.

In principle, one can obtain improved accuracy by using a larger *cluster* of cells, and appropriately enlarging the parameter space to include additional fugacities for longer-range links joining further-neighbor monomers (see, e.g.,

[7.100]). These additional parameters are required to maintain the proper *inter-cell* correlations upon rescaling. This approach is somewhat cumbersome because the number of parameters quickly becomes very large. To improve the accuracy of the small-cell calculation, but still maintain the simplicity of the one-parameter approach, it is natural to consider using larger cells, as was discussed in the section on percolation.

With all our weight functions, configurations within the cell are accounted for to a good approximation, but connection of chains between cells is treated inaccurately. While it seems this should introduce an error proportional to the surface-to-volume ratio of the cell, it is not clear whether this is literally the case. Nevertheless the results of the closed-form position-space renormalization group with small cells do indicate a trend toward the "correct" asymptotic limit [7.98].

b) *Extensions*

1) Large Cells. Based on the trend in the small-cell results and on the analogy with percolation, the above approach has been extended to large cells using a "constant fugacity" Monte Carlo method in which K, the bond fugacity, is the basic parameter as opposed to the number of steps N used in conventional simulation methods [7.98]. Through this approach, chains of order 10^3 bonds can be simulated in an a priori unbiased fashion on the square lattice with only moderate use of computer time. The efficiency of this method compares well with standard methods of Monte Carlo simulation of chains [7.45,46].

By this method, the recursion relation for toroidal cells with b up to 150 were studied (Table 7.2). By extrapolating the sequence of estimates according to (7.16b), one obtains the estimate $\nu = 0.756 \pm 0.004$. This value may be compared with (7.2), the Flory approximation $\nu_F = 3/4$. It is not clear whether the present results are sufficiently reliable to safely exclude the Flory value. For example, the sequence $\nu(b)$ obtained using the first weight function we discussed—the corner rule—is not monotonic; hence it is not clear that the toroidal cell results are correct just because they *are* monotonic!

2) Three-Dimensional Systems. The above procedure can be readily extended to any dimension, with a corresponding increase in the labor of calculating the recursion relation K'(K). The corner rule has been used [7.101] to study the d = 3 simple cubic lattice for b = 2 and 3. For b = 2,

$$K'(K) = 10K^8 + 16K^7 + 14K^6 + 12K^5 + 8K^4 + 4K^3 + K^2 \quad . \tag{7.27}$$

The nontrivial fixed point is at $K^* = 0.297$, which may be compared to the most reliable estimate $K_c = 1/\mu = 0.2135 \pm 0.0001$ [7.102]. The eigenvalue obtained from (7.27) results in the prediction $\nu = 0.588$, which agrees precisely with the highly accurate field theory prediction $\nu = 0.588 \pm 0.0015$ [7.103], and with the value

Table 7.2. An example of Monte Carlo renormalization group results. The sequence shown is for the case of linear polymers (toroidal rule). Similar sequences exist for percolation [Ref.7.44, Tables 7,8]. In the large cell results, the numbers in parenthesis give the uncertainty in the last decimal place shown. Note the convergence toward accurate extrapolated results. Adapted from [7.98]

(a) cell-to-bond

b	K^*	ν
2	0.3660	0.6897
3	0.3707	0.7050
4	0.3725	0.7122
5	0.3734	0.7165
10	0.3756(3)	0.7258(1)
20	0.3768(2)	0.7318(1)
40	0.3779(1)	0.7360(3)
80	0.3784(1)	0.7400(7)
150	0.3787(1)	0.7417(5)
extrapolation	0.3791(1)	0.756(4)

(b) cell-to-cell

b'/b	K^*	ν
2/1	0.3660	0.6897
3/2	0.3747	0.7329
4/3	0.3754	0.7412
5/4	0.3759	0.7443
extrapolation	0.3791	0.755

$\nu = 0.586 \pm 0.004$ [7.104] obtained from careful re-analysis of much of the existing experimental data. Of course, this accurate agreement may only be coincidental. In fact, when one extends the calculation to b = 3 [7.101], one finds that although $K^* = 0.276$ is closer to the series estimate, $\nu = 0.581$ is somewhat less remarkable. Additional results using larger cells and other weight functions are clearly needed.

3) Cell-to-Cell Transformation. Following the spirit of the percolation problem, one can also derive a cell-to-cell transformation in which a cell of edge b is rescaled to a cell of edge b'. The results of such a cell-to-cell transformation, with b'/b = 6/5, give values comparable in accuracy to a cell-to-bond transformation with $b \sim 100$ [7.98]. This is similar to the increase in accuracy achieved in percolation using the cell-to-cell transformation. Furthermore, extrapolating the d = 2 cell-to-cell results versus ln b/b', yields values for ν in the vicinity of 0.755 depending on the weight function used. These numbers agree quite well with the large-cell extrapolation using the toroidal rule.

4) The $b \to 1$ Limit. Although it is not in general possible to calculate recursion relations in closed form for arbitrary b and d, progress can be made if we take the limit $b \to 1$. A similar approach for percolation was considered by SHAPIRO [7.105,106]. For example, for the corner rule, one obtains a lower bound to K' by noting that there is at least one SAW of any length $n > b$ which can span the

cell. Thus [7.98]

$$K'_{\text{lower bound}} = \sum_{n=b}^{b^d} K^n < K'_{\text{exact}} \quad . \tag{7.28a}$$

Similarly, an upper bound is obtained by noting that the number of spanning n-step SAWs is bounded by an exponential. That is,

$$K'_{\text{upper bound}} = \sum_{n=b}^{b^d} b^{n-b} K^n > K'_{\text{exact}} \quad . \tag{7.28b}$$

The sums in (7.28) can both be evaluated, and as $b \to 1$, they become identical:

$$K'_{\text{inf}} = K + (b - 1)(1 - Kd)K(\ln K)/(1 - K) \quad . \tag{7.29}$$

This transformation, of course, still contains vestiges of the approximation inherent in the finite-cell approach. From this recursion relation, one finds

$$\nu = (d - 1)/(d \ln d) \quad . \tag{7.30}$$

This formula provides fairly reasonable results: $\nu = 1$, 0.721, 0.607, and 0.541 in $d = 1,2,3$, and 4 respectively.

Transformations obtained in this way for *percolation* [7.65,106] are identical to the Migdal-Kadanoff renormalization-group recursion relations, which are exact in $d = 1$; likewise, the cell approach is exact in $d = 1$. Thus, for $d \to 1$ (7.30) may also be exact. To first order in $\varepsilon = d - 1$, (7.30) gives $\nu = 1 - \varepsilon/2$. In contrast, the Flory formula (7.2) gives $\nu_F = 1 - \varepsilon/3$. Thus, just as for $d = 4 - \varepsilon$ [7.5], the Flory formula appears to give too large a value for ν.

7.3.3 Lattice Animals

a) *Basic Approach*

The generating function for lattice animals (7.9) is formally like the generating function (7.6) for SAWs, except that A_L now includes *all* configurations of connected clusters. Hence to formulate a position-space renormalization group for lattice animals, one need only follow the arguments of the previous section, replacing SAWs by lattice animals in the configurations we sum over. For the square lattice with $b = 2$, one finds for bond animals [7.97]

$$K' = K^8 + 8K^7 + 21K^6 + 24K^5 + 14K^4 + 4K^3 + K^2 \quad . \tag{7.31}$$

The fixed point of this transformation is at $K = 0.270$, which may be compared with the result $1/\mu = 0.192 \pm 0.002$ [7.48]. The corresponding exponent characterizing the singularity in the mean "animal" radius is $\nu = 0.571$, which is smaller than the values 0.61 obtained by PARISI and SOURLAS [7.10] and 0.625 obtained by ISAACSON and LUBENSKY [7.8] using a Flory approach.

Table 7.3. The exponent ν and the threshold parameter K_c for d = 2 SAWs (linear polymers) and lattice animals (branched polymers). The upper number is the estimated ν, obtained from the direct position-space renormalization group (PSRG) described in Sects.7.3.2,3. The lower number, in parenthesis, is the prediction for the threshold parameter K_c. Adapted from [7.97]

	Direct PSRG	Other methods
Linear	0.756 ± 0.004[a] (0.3791 ± 0.0001)	0.74 - 0.75[c] (0.3790[d])
Branched	0.627[b]	0.61 - 0.65[e]
(with loops)	(0.254)	(0.192[f])

[a]Extrapolation of b = 2 - 150 results (cf. Table 7.2) [7.98]; [b]a cell-to-cell transformation with $b_1 = 3$, $b_2 = 2$ [7.97]; [c]FLORY [7.2] ($\nu = 0.75$); KREMER et al. [7.107] ($\nu = 0.74 \pm 0.01$); DERRIDA [7.99] ($\nu = 0.7503 \pm 0.0002$); [d]SYKES et al. [7.47]; [e]ISAACSON and LUBENSKY [7.8] ($\nu = 0.625$); PARISI and SOURLAS [7.10] ($\nu = 0.61$); GOULD and HOLL [7.108] ($\nu = 0.65 \pm 0.02$); DERRIDA and de SEZE [7.109] ($\nu = 0.6408 \pm 0.0003$); [f]SYKES and GLEN [7.48]

The discrepancy becomes smaller when one calculates K'(K) for b = 3: K^* increases to 0.261, and ν increases to 0.593. A cell-to-cell transformation based on the b = 2 and b = 3 calculations gives $K^* = 0.254$ and $\nu = 0.627$ (cf. Table 7.3).

Excluding loop formation leads to a recursion relation analogous to (7.31). The corresponding exponent ν differs so little from the value obtained from the full recursion relation [7.97], that it lends support to the prediction from field theoretical calculations that branched polymers with and without loops belong to the same universality class [7.11].

b) *Extensions*

1) Crossover Between SAWs and Lattice Animals. Given the parallels between the treatment of the SAW and lattice animal problems, it is tempting to incorporate both problems in a single two-parameter model. Let K be the monomer fugacity as before, and let f represent the probability that a randomly chosen site on a polymer is a polyfunctional unit (i.e., that this site is free to have more than two bonds "branching out" from it). One obtains *coupled* recursion relations [7.97] of the form,

$$K' = K'(K,f) \quad , \tag{7.32a}$$

$$f' = f'(K,f) \quad . \tag{7.32b}$$

This two-parameter position-space renormalization group transformation may be solved numerically for the fixed points, critical surface, and critical exponents [7.97]. The global flow diagram is sketched in Fig.7.14a for the special case of no loops. Note that there is a critical fixed point with f = 0 that is clearly identifiable

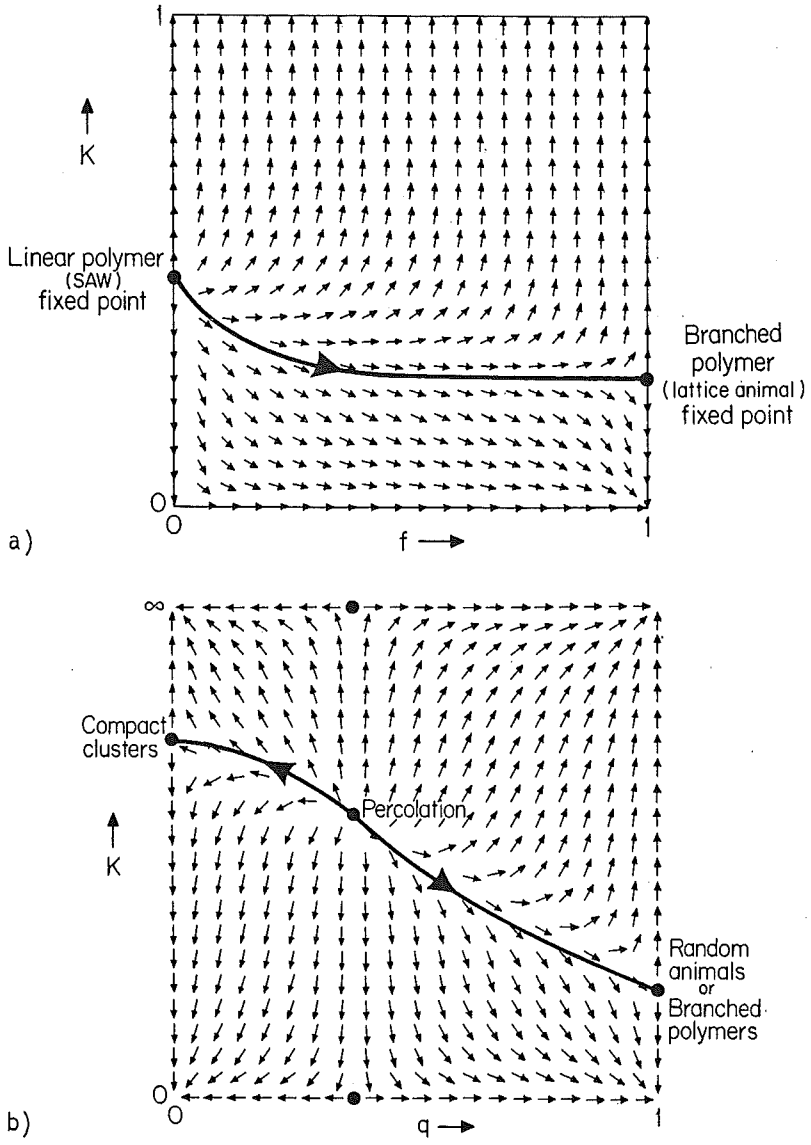

Fig.7.14. (a) Flow diagram showing crossover from SAWs to lattice animals as f, the probability of a polyfunctional unit, is varied. It is seen that SAWs and lattice animals belong to different universality classes. When $f > 0$, the flow is to the lattice animal fixed point. (b) Flow diagram for the crossover between lattice animals, percolation, and compact clusters, the 3 limits of the generalized animal problem cf. (7.33) . At $q = 0$, only clusters with the smallest possible perimeters contribute (compact clusters), while at $q = 1$ all lattice animals contribute equally (the "random animal" limit). Finally, along the line $q = 1 - K$, one obtains the percolation problem. The flow diagram suggests that these 3 cases belong to 3 separate universality classes. The percolation point is a multicritical point from which the flow is to the random animal fixed point for $q > q_c$, and to the compact cluster point for $q < q_c$. Adapted from [7.15,97]

as the SAW fixed point since no branching is allowed, and a second critical fixed point with $f = 1$, that corresponds to a structure that is fully branched. Additionally, for any amount of branching, no matter how small, the flow is toward the latter fixed point. Physically, this suggests that when even a few cross-linking units are

present, polymeric systems obey the statistics of fully branched polymers. However, SAWs and lattice animals belong to two different universality classes. By following the flow trajectory from the SAW fixed point toward the lattice animal fixed point, one obtains the critical surface—shown as a solid line in Fig.7.14a.

This result agrees with a "blob" picture of randomly branched polymers [7.9]. The introduction of cross-linking units imposes a length scale, R_{blob}, defined by the mean separation between the cross links. One can thereby consider "effective monomers" of diameter, R_{blob} undergoing polyfunctional condensation. Thus for distance scales larger than R_{blob}, one expects to observe the asymptotic behavior of branched polymers.

2) Crossover Between Lattice Animals and Percolation. Consider the generalized generating function [7.15]

$$G(K,q) = \sum_{\text{config}} c(L,t)\, K^L q^t \quad , \tag{7.33}$$

where q may be considered an arbitrary parameter. Here the summation is over all configurations of the desired topological type, having L bonds and t perimeter bonds. The topological type is specified by the particular configurations included in c(L,t). Depending on the weight q assigned to the perimeters, branched configurations with different statistics will occur [7.15]. Both the SAW and lattice animal problems can be obtained in the limit that the fugacity for perimeter bonds, q, is unity. Furthermore, if K is identified with the bond occupation probability, and q = 1 - K, then G(K,q) is identical to the generating function for the bond percolation problem.[10] Thus we can calculate the statistical properties [cf., e.g., (7.1)] of percolation clusters and other "general nonrandom animals" (i.e., q ≠ 1) equally readily using the direct position-space renormalization group.

To illustrate this in terms of a site description, a renormalized cell now plays the role of either an interior (occupied) site or a perimeter (empty) site; here we formulate the discussion in terms of site animals, but the same procedure is equally applicable for bond animals. Each *site* in an animal is weighted by a fugacity K, and an occupied *cell* has a fugacity K'. In addition, perimeter sites receive a weight q, and a cell "occupied" by a perimeter site receives weight q'. To write the recursion relations for K' and q' we must define a rule for when a cell is occupied. If a cell is occupied when a cluster spans the cell in both horizontal and vertical directions (this rule is called R_2 in [7.44]), then the recursion relation for K is

$$K' = K^4 + 4K^3 q \quad . \tag{7.34a}$$

---

10 In this case, limiting c(L,t) to SAWs would result in a "restricted valence" percolation problem ([7.110] and references therein) in which lattice animals with more than two occupied bonds incident upon a given site, or with ring closures, are forbidden.

To renormalize q, we treat it as a probability that a site is empty (as in percolation) and write

$$q' = q^4 + 4q^3(1 - q) + 6q^2(1 - q)^2 \quad . \tag{7.34b}$$

Note that q is an independent variable in (7.34), i.e., $q \neq 1 - K$ in contrast to the percolation recursion relation. However, if $q = 1 - K$, the two equations are consistent, and they reduce to the recursion relations for percolation under rule R_2.

The coupled recursion relations (7.34a,b) constitute a two-parameter position-space renormalization group transformation for the "generalized animal" problem. Nine fixed points are found, as indicated schematically in the flow diagram of Fig.7.14b. The three *critical* fixed points are indicated by heavy dots. The most unstable fixed point is the "percolation fixed point" where $q = 1 - K$. If the system is initially on the critical surface near the percolation fixed point, it flows under successive renormalizations to either the "random lattice-animal fixed point" at $q = 1$ or to the "compact cluster fixed point" at $q = 0$. The critical behavior below p_c is governed by the random animal fixed point, while the critical behavior above p_c is controlled by the compact cluster fixed point. This procedure has been used [7.15] to confirm earlier conjectures of various workers [7.30] that the critical exponent ν (called ρ in much of the literature) governing the dependence of the mean diameter on the degree of polymerization should be a discontinuous function of p, taking on the random animal value for all $p < p_c$, the percolation value at $p = p_c$, and the compact cluster value for $p > p_c$.

The corresponding numerical values of the exponent ν may be calculated by computing the matrix of derivatives

$$T = \begin{pmatrix} \partial K'/\partial K & \partial K'/\partial q \\ \partial q'/\partial K & \partial q'/\partial q \end{pmatrix}_{K = K^*,\ q = q^*} \quad . \tag{7.35}$$

Since $\partial q'/\partial K = 0$, the eigenvalues of this matrix are simply

$$\lambda_K = \partial K'/\partial K|_{K^*,q^*} = 4K^3 + 12K^2 q|_{K^*,q^*} \tag{7.36a}$$

and

$$\lambda_q = \partial q'/\partial q|_{K^*,q^*} = 12q^3 - 24q^2 + 12q|_{K^*,q^*} \quad . \tag{7.36b}$$

The exponent ν is given by $\ln b/\ln\lambda_K$, while ν_p, the percolation connectedness length exponent, would be obtained from this *same* expression if $q = 1 - K$ in (7.34a). This, however, is equivalent to (7.34b). Thus $\nu_p = \ln b/\ln\lambda_q$. The numerical values of the exponents are given in Table 7.4. In particular, we note that the result $\nu = 0.52 \pm 0.02$ at p_c has recently been obtained using the above approach by extrapolation of results for $b \leq 5$ [7.111].

Table 7.4. Results for the generalized animal problem, based on direct position-space renormalization group calculations on the square lattice using the smallest cell (b = 2). Best estimates for the exponents ν and ν_p are given in square brackets (see also Fig.7.14b)

	(K^*,q^*)	ν	ν_{perc}
Branched polymer (Random animal)	(0.47,1)	0.61 [0.61 - 0.65][a]	-
Percolation	(0.77,0.23)	0.56 [0.52 - 0.53][b]	1.39 [4/3][c]
Compact	(1,0)	1/2 [1/2][d]	-

[a]ISAACSON and LUBENSKY [7.8]; PARISI and SOURLAS [7.10]; FAMILY [7.97]; [b]GOULD and HOLL [7.108]; FAMILY and REYNOLDS [7.111]; [c]BLACK and EMERY [7.69]; NIENHUIS [7.70]; [d]Exact

7.4 Other Approaches

For reasons of clarity, we have presented one main avenue of approach to position-space renormalization group in percolation and polymers. It has the advantage that the same approach works for many different lattice statistical problems. Other approaches which show promise have also been recently initiated. We shall devote this concluding section to a brief discussion of some of these.

7.4.1 Percolation

For percolation, YOUNG and STINCHCOMBE [7.62] initiated the use of a decimation transformation as mentioned in Sect.7.3.1. This has the advantage of simplicity, but the drawback that thus far it has been largely a "single-shot" technique with no systematic method of gauging the magnitude of the errors introduced by the method.

Phenomenological renormalization [7.99,109,112,113] holds promise for providing extremely accurate estimates of critical parameters because, like the cell-to-cell approach, the convergence seems to be linear in 1/b, rather than in 1/ln b [cf. (7.16b)]. Moreover, fairly large b can be treated; currently, extrapolations are based on up to 10 exact data points. While the phenomenological renormalization approach gives impressive numerical results, it cannot be easily adapted to a multi-parameter rescaling. In contrast, the cell renormalization discussed above can be easily generalized to more parameters in order to treat crossover phenomena and global phase diagrams (see, e.g., Sect.7.3.3). The phenomenological method has been discussed in Chap.3 and so will not be further described here.

7.4.2 Self-Avoiding Walks

It was remarked above that the initial position-space renormalization group calculations for percolation utilized the Q-state Potts Hamiltonian and subsequently took the $Q \to 1$ limit to recover percolation properties. Similarly, the first position-space renormalization group calculations for SAWs utilized a discrete version of the "n-vector model" and subsequently took the $n \to 0$ limit ([7.114]; for a generalization of this model designed to model branched polymers see [7.115]).

Possible "direct" position-space renormalization group calculations that do *not* require using a Hamiltonian have been suggested by several authors [7.1,95-99]. The cell approach [7.96-98] has been described above because it is conceptually analogous to the approach used for both percolation and lattice animals. Now we briefly describe the other "direct" position-space renormalization group treatments of SAWs.

SHAPIRO [7.95] was the first to apply a decimation procedure directly on the SAW generating function. This was a very useful conceptual advance. NAPIÓRKOWSKI et al. [7.100] considered a cell position-space renormalization group using a second-order cumulant-like approximation requiring five parameters. They obtained $\nu = 0.712$ and 0.769 on the square and triangular lattices respectively. MALAKIS [7.116], following NAPIÓRKOWSKI et al., used a decimation technique with several parameters.

De GENNES [7.1] has suggested a variation of decimation that he terms "decimation along the chain". This general approach has been implemented and extended with good results. BAUMGÄRTNER [7.117] has used a Monte Carlo renormalization group version of it to obtain $\nu = 0.586 \pm 0.004$ for a *continuum* model of a $d = 3$ polymer. However, more extensive work based on this method [7.107] has given error bars on ν which include the Flory value $\nu = 3/5$. Thus in three dimensions, it appears that ν may be less than 0.6, although the issue does not seem completely resolved. For $d = 2$ KREMER et al. [7.107] found $\nu = 0.74 \pm 0.01$ based on an extensive study using this Monte Carlo renormalization method.

The highest claimed accuracy for $d = 2$ is due to DERRIDA [7.99], who has applied extrapolation ideas to a phenomenological renormalization procedure. On the square lattice with periodic boundary conditions, he obtained $\nu = 0.7503 \pm 0.0002$. However, his results have the same non-monotonicities as the large-cell SAW approach described above, in the case of cells with free boundary conditions. We raise here the same question as we raised previously: Just because the results with a particular weight function appear monotonic, are they therefore correct?

7.4.3 Lattice Animals

Very recently, the phenomenological renormalization approach has been extended to *site* lattice animals on a square lattice [7.109]. The extrapolated estimate $\nu = 0.6408 \pm 0.0003$ agrees well with estimates obtained by other methods. There is no position-space renormalization group work on *bond* animals other than that discussed in Sect.7.3.3.

7.5 Concluding Remarks and Outlook

In this chapter, we have focused on the application of a relatively simple approach—use of a "connectivity" weight function—to the description of critical phenomena occurring in three mathematical models of polymer systems. It is perhaps appropriate to conclude by emphasizing the generality of the connectivity approach.

Not surprisingly, this approach can be used to treat a wide range of problems for which the basic physics is "connectivity"—ranging from simple models such as those described in this chapter, to more complex models like those used to describe physical phenomena such as vulcanization [7.118,119], directed percolation [7.120-127], anisotropic percolation [7.128-131], second-neighbor percolation [7.129,132,133], site-bond percolation [7.31-33], correlated percolation [7.134,135], time-dependent percolation [7.108], and the related problem of "growing lattice animals" [7.136].

Perhaps more surprisingly, the connectivity approach can be extended to treat lattice statistical models for which connectivity does not at first sight appear to be the appropriate physical concept. For example, the essential physics underlying the thermal behavior of an Ising model is not obviously connectivity, yet we know that there are striking analogies between the Ising model behavior near T_c and percolation phenomena near p_c (see Fig.7.15). Recently, TSALLIS and his collaborators [7.138,139] have proposed an ingenious approach to the Ising and q-state Potts models which focuses upon the "transmission" of correlation through the bonds. They use the self-dual bond cells illustrated in Fig.7.12 rather than the more conventional Kadanoff construction using site cells. In this fashion they have constructed an Ising-model renormalization group, using connectivity weight functions, that correctly predicts the exact critical point for all finite-size cells.

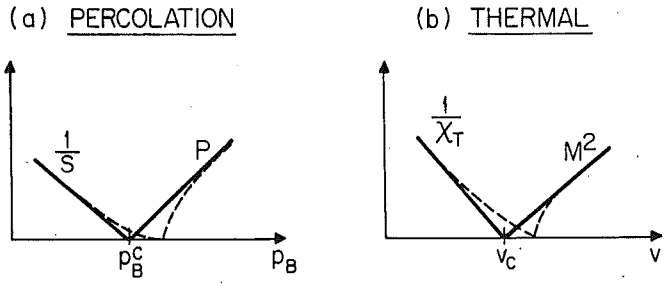

Bond probability p_B^c = percolation pt.	Coupling constant $v_c = \tanh(J/kT_c)$
Bond cluster	Droplet
P(p) S(p)	M χ_T
$<N_{clusters}>$	G(H,T)
Fisher-Essam $d_c = 6$	Husimi-Temperley $d_c = (2\beta+\gamma)/\nu = 4$

Fig.7.15a,b. Illustration of the analogies between (a) bond percolation, and (b) an ordinary thermal phase transition (e.g., an Ising or lattice-gas model). Adapted from [7.137]. As discussed in Sect.7.5, the same connectivity approach used in percolation can be extended to the "thermal transmissivity" of the magnetic system

While we have not emphasized the generality of the connectivity approach, we have tried to emphasize the extent to which the "one-cell, one-parameter renormalization group" can attain high accuracy by considering successively larger cells. Thus while other position-space renormalization group approaches include more parameters in an effort to obtain better accuracy, this approach focuses upon using larger cells. The advantage of our approach is that there is a well-defined procedure for extrapolating a sequence of approximate results. The outcomes of such extrapolations give numerical agreement with exact information where available.

There is one circumstance where it is desirable—and feasible—to include additional parameters. This occurs when one wishes to study crossover between universality classes. Such studies were illustrated above in Sect.7.3.3 when we discussed the crossover between linear and branched polymers, and the crossover between branched polymers and percolation. One may thereby determine if an additional parameter is relevant or irrelevant. Thus, e.g., site percolation and bond percolation can be clearly demonstrated to belong to the same universality class [7.32,33]. Four-coordinated correlated percolation [7.140] and random percolation can be similarly shown to be in the same universality class [7.135]. In these cases, the additional parameter which was introduced was an irrelevant variable. On the other hand, e.g., directed ("diode") percolation and random percolation can clearly be seen to belong to different universality classes [7.122], and the additional variable is relevant.

Acknowledgements. Some of the work described here was carried out in collaboration with other members of our research group, including Antonio Coniglio, Agustin E. Gonzalez, Harvey Gould, William Klein, Hisao Nakanishi, and Gerald Shlifer. We are particularly indebted to sustained interactions with our distinguished visitors, especially Professors Kurt Binder, Pierre-Gilles de Gennes, Dietrich Stauffer, and Constantino Tsallis, who have generously shared with us their interest and enthusiasm. Finally, we wish to thank Bernard Derrida and Robin Stinchcombe for continuing to send us copies of their groups' work prior to publication. Also, we wish to apologize to these and perhaps other authors for the fact that space—and considerations of pedagogy—do not permit a fuller exposition of their important contributions to this field.

References

7.1 P.G. de Gennes: *Scaling Concepts in Polymer Physics* (Cornell Univ. Press, Ithaca 1979); Riv. Nuovo Cimento *7*, 363 (1972)
7.2 P.J. Flory: *Principles of Polymer Chemistry* (Cornell Univ. Press, Ithaca 1953)
7.3 M.E. Fisher: J. Phys. Soc. Jpn (Suppl.) *26*, 44 (1969)
7.4 J. des Cloiseaux: J. Phys. Paris *37*, 431 (1976)
7.5 P.G. de Gennes: Phys. Lett. *38A*, 339 (1972)
7.6 H.E. Stanley: Phys. Rev. Lett. *20*, 489 (1968)
7.7 M. Daoud, J.P. Cotton, B. Farnoux, G. Jannink, G. Sarma, H. Benoit, R. Duplessix, C. Picot, P.G. de Gennes: Macromolecules *8*, 804 (1975)

7.8 J. Isaacson, T.C. Lubensky: J. Phys. Paris Lett. *41*, L469 (1980)
7.9 M. Daoud, J.F. Joanny: J. Phys. Paris *42*, 1359 (1981)
7.10 G. Parisi, N. Sourlas: Phys. Rev. Lett. *46*, 871 (1981)
7.11 T.C. Lubensky, J. Isaacson: Phys. Rev. A*20*, 2130 (1979)
7.12 P.G. de Gennes: C.R. Acad. Sci. *291*, 17 (1980)
7.13 A.B. Harris, T.C. Lubensky: Phys. Rev. B*24*, 2656 (1981)
7.14 F.Y. Wu: Rev. Mod. Phys. *54*, 235 (1982)
7.15 F. Family, A. Coniglio: J. Phys. A*13*, L403 (1980)
7.16 H.E. Stanley: In *Festschrift for Laszlo Tisza*, ed. by A. Shimony, H. Feshbach (MIT Press, Cambridge 1982)
7.17 A.B. Harris, T.C. Lubensky, W.K. Holcomb, C. Dasgupta: Phys. Rev. Lett. *35*, 327 (1975)
7.18 R.G.Priest, T.C. Lubensky: Phys. Rev. B*13*, 4159 (1976)
7.19 D.J. Amit: J. Phys. A*9*, 1441 (1976)
7.20 M. Gordon, S.B. Ross-Murphy: Pure Appl. Chem. *43*, 1 (1975)
7.21 T. Vicsek, J. Kertêsz: J. Phys. A*14*, L31 (1981)
7.22 E.T. Gawlinski, H.E. Stanley: J. Phys. A*14*, L291 (1981); S.W. Haan, R. Zwanzig: J. Phys. A*10*, 1547 (1977)
7.23 P.J. Flory: J. Am. Chem. Soc. *63*, 3083 (1941)
7.24 W.H. Stockmayer: J. Chem. Phys. *12*, 125 (1944)
7.25 M.E. Fisher, J.W. Essam: J. Math. Phys. *2*, 609 (1961)
7.26 H.L. Frisch, J.M. Hammersley: SIAM J. Appl. Math. *11*, 894 (1963)
7.27 P.G. de Gennes: J. Phys. Paris *36*, 1049 (1975)
7.28 D. Stauffer: J. Chem. Soc. Faraday Trans. II *72*, 1354 (1976)
7.29 D. Stauffer, A. Coniglio, M. Adam: Adv. Ply. Sci. *44*, 103 (1982)
7.30 D. Stauffer: Phys. Rep. *54*, 1 (1979)
7.31 P. Agrawal, S. Redner, P.J. Reynolds, H.E. Stanley: J. Phys. A*12*, 2073 (1979)
7.32 H. Nakanishi, P.J. Reynolds: Phys. Lett. *71*A, 252 (1979)
7.33 B. Shapiro: J. Phys. C*12*, 3185 (1979)
7.34 A. Coniglio, H.E. Stanley, W. Klein: Phys. Rev. Lett. *42*, 518 (1979)
7.35 A. Coniglio, H.E. Stanley, W. Klein: Phys. Rev. B*25*, 6805 (1982)
7.36 T. Tanaka, G. Swislow, A. Ohmine: Phys. Rev. Lett. *42*, 1556 (1979)
7.37 A.E. Gonzales, M. Daoud: J. Phys. A*14*, 2441 (1981)
7.38 A.E. Gonzales, S. Muto: J. Chem. Phys. *73*, 4668 (1980)
7.39 M. Schmidt, W. Burchard: Macromolecules *14*, 370 (1981)
7.40 C. Domb: J. Phys. A*9*, 283 (1976)
7.41a H.E. Stanley: J. Phys. A*10*, L211 (1977);
7.41b A. Coniglio: Phys. Rev. Lett. *46*, 250 (1981); Preprint (1981)
7.41c R. Pike, H.E. Stanley: J. Phys. A*14*, L169 (1981)
7.42 P.J. Reynolds, W. Klein, H.E. Stanley: J. Phys. C*10*, L167 (1977)
7.43 P.J. Reynolds, H.E. Stanley, W. Klein: J. Phys. A*11*, L199 (1978)
7.44 P.J. Reynolds, H.E. Stanley, W. Klein: Phys. Rev. B*21*, 1223 (1980)
7.45 C. Domb: Adv. Chem. Phys. *15*, 229 (1969)
7.46 D.S. McKenzie: Phys. Rep. *27*C, 35 (1976)
7.47 M.F. Sykes, A.J. Guttman, M.G. Watts, P.D. Roberts: J. Phys. A*5*, 653 (1972)
7.48 M.F. Sykes, M. Glen: J. Phys. A*9*, 87 (1976)
7.49 D.S. Gaunt: J. Phys. A*13*, L97 (1980)
7.50 J. Hoshen, D. Stauffer, G.H. Bishop, R.J. Harrison, G.B. Quinn: J. Phys. A*12*, 1285 (1979)
7.51 H. Nakanishi, H.E. Stanley: J. Phys. A*11*, L189 (1978); Phys. Rev. B*22*, 2466 (1980); J. Phys. A*14*, 693 (1981)
7.52 J.W. Essam: Rep. Prog. Phys. *43*, 833 (1980)
7.53 P.J. Reynolds, H.E. Stanley, W. Klein: J. Phys. A*10*, L203 (1977)
7.54 D.S. Gaunt, H. Ruskin: J. Phys. A*11*, 1369 (1978)
7.55 D.S. Gaunt, M.F. Sykes, H. Ruskin: J. Phys. A*9*, 1899 (1976)
7.56 T.D. Lee, C.N. Yang: Phys. Rev. *87*, 410 (1952)
7.57 R.B. Potts: Proc. Cambridge Philos. Soc. *48*, 106 (1952)
7.58 P. Kasteleyn, C.M. Fortuin: J. Phys. Soc. Jpn (Suppl.) *26*, 11 (1969)
7.59 D.J. Amit, D.J. Wallace, R.K.P. Zia: Phys. Rev. B*15*, 4657 (1977)
7.60 C. Dasgupta: Phys. Rev. B*14*, 1221 (1976)

7.61 T.S. Burkhardt, B.W. Southern: J. Phys. A*11*, L253 (1975)
7.62 A.P. Young, R.B. Stinchcombe: J. Phys. C*8*, L535 (1975); *9*, L643 (1976)
7.63 L.G. Marland, R.P. Stinchcombe: J. Phys. C*10*, 2223 (1977)
7.64 L.G. Marland: J. Phys. C*11*, L617 (1978)
7.65 S. Kirkpatrick: Phys. Rev. B*15*, 1533 (1977)
7.66 A.A. Migdal: Sov. Phys. JETP *42*, 413; 743 (1975)
L.P. Kadanoff: Ann. Phys. (N.Y.) *100*, 359 (1976)
7.67 Z. Djordjevic, H.E. Stanley, A. Margolina: J. Phys. A*15* (1982)
M.F. Sykes, D.S. Gaunt, M. Glen: J. Phys. A*9*, 97 (1976)
7.68 M.P.M. den Nijs: J. Phys. A*12*, 1857 (1979)
7.69 J.L. Black, V.J. Emery: Phys. Rev. B*23*, 429 (1981)
7.70 B. Nienhuis: J. Phys. A*15*, 199 (1982)
7.71 Z. Friedman, J. Felsteiner: Phys. Rev. B*15*, 5317 (1977)
7.72 M.E. Fisher: In *Critical Phenomena*, ed. by M.S. Green (Academic, New York 1971);
A. Sur, J.L. Lebowitz, J. Marro, M.L. Kalos, S. Kirkpatrick: J. Stat. Phys. *15*, 145 (1976)
7.73 E. Brézin: J. Phys. Paris *43*, 15 (1982)
7.74 P.D. Eschbach, D. Stauffer, H.J. Herrmann: Phys. Rev. B*23*, 422 (1981)
7.75 J. Hoshen, R. Kopelman: Phys. Rev. B*14*, 3438 (1976)
7.76 R.B. Pearson: Phys. Rev. B*22*, 2579 (1980)
7.77 B. Nienhuis, E.K. Riedel, M. Schick: J. Phys. A*13*, L189 (1980)
7.78 J. Bernasconi: Phys. Rev. B*18*, 2185 (1978)
7.79 S. Kirkpatrick: In *Ill-Condensed Matter*, ed. by R. Balian, R. Maynard, G. Toulouse (North Holland, Amsterdam 1979)
7.80 C.J. Lobb, K.R. Karasek: J. Phys. C*13*, L245 (1980);
C.J. Lobb, K.R. Karase: Phys. Rev. B*25*, 492 (1982)
7.81 A.C.N. de Magalhães, C. Tsallis, G. Schwachheim: J. Phys. C*13*, 321 (1980)
7.82 D.W. Heermann, D. Stauffer: Z. Phys. B*40*, 113 (1981); Preprint (1981)
7.83 Y. Yuge: J. Phys. A*12*, 2509 (1979); Phys. Rev. B*18*, 1514 (1978)
7.84 A.G. Dunn, J.W. Essam, D.S. Ritchie: J. Phys. C*8*, 4219 (1975)
7.85 R. Rosman, B. Shapiro: Phys. Rev. B*16*, 5117 (1977)
7.86 R.B. Stinchcombe, B.P. Watson: J. Phys. C*9*, 3221 (1976)
7.87 C.J. Lobb, D.J. Frank: J. Phys. C*12*, L827 (1979);
AIP Conf. Proc. *58*, 308 (1980);
C.J. Lobb, D.J. Frank, M. Tinkham: Phys. Rev. B*23*, 2262 (1981)
7.88 H. Kunz, B. Payandeh: Phys. Rev. B*20*, 1285 (1979)
7.89 R. Fisch, A.B. Harris: Phys. Rev. B*18*, 416 (1978)
7.90 G. Shlifer, W. Klein, P.J. Reynolds, H.E. Stanley: J. Phys. A*12*, L169 (1979)
7.91 S. Kirkpatrick: AIP Conf. Proc. *40*, 99 (1978)
7.92 R. Pike, H.E. Stanley: J. Phys. A*14*, L169 (1981)
7.93 W. Kinzel: Z. Phys. B*34*, 79 (1979)
7.94 H.E. Stanley, R.J. Birgeneau, P.J. Reynolds, J.F. Nicoll: J. Phys. C*9*, L553 (1976)
7.95 B. Shapiro: J. Phys. C*11*, 2829 (1978)
7.96 S.L.A. de Queiroz, C.M. Chaves: Z. Phys. B*40*, 99 (1980)
7.97 F. Family: J. Phys. A*13*, L325 (1980)
7.98 S. Redner, P.J. Reynolds: J. Phys. A*14*, 2679 (1981); *14*, L55 (1981)
7.99 B. Derrida: J. Phys. A*14*, L5 (1981)
7.100 M. Napiórkowski, E.M. Hauge, P.C. Hemmer: Phys. Lett. *72A*, 193 (1979)
7.101 F. Family: J. Phys. Paris *42*, 189 (1981)
7.102 M.G. Watts: J. Phys. A*8*, 61 (1975)
7.103 J.C. le Guillou, J. Zinn-Justin: Phys. Rev. B*21*, 3976 (1980)
7.104 J.P. Cotton: J. Phys. Lett. Paris *41*, L231 (1980)
7.105 B. Shapiro: J. Phys. C*11*, L863 (1978)
7.106 B. Shapiro: J. Phys. C*13*, 3387 (1980)
7.107 K. Kremer, A. Baumgärtner, K. Binder: Z. Phys. B*40*, 331 (1981)
7.108 H. Gould, K. Holl: J. Phys. A*14*, L443 (1981)
7.109 B. Derrida, L. de Seze: J. Phys. Paris *43*, 475 (1982)
7.110 J. Kertész, B.K. Chakrabarti, J.A.M.S. Duarte: J. Phys. A*15*, L13 (1982);
S.G. Whittington, K.M. Middlemiss, D.S. Gaunt: J. Phys. A*14*, 2415 (1981);

S.G. Whittington, K.M. Middlemiss, G.M. Torrie, D.S. Gaunt: J. Phys. A*13*, 3707 (1980);
R. Cherry, C. Domb: J. Phys. A*13*, 1325 (1980);
D.S. Gaunt, J.L. Martin: G. Ord, G.M. Torrie, S.G. Whittington: J. Phys. A*13*, 1791 (1980)
7.111 F. Family, P.J. Reynolds: Z. Phys. B*45*, 123 (1981)
7.112 M.P. Nightingale: Proc. K. Ned. Ak. Wet. B*82*, 235 (1979)
7.113 B. Derrida, J. Vannimenus: J. Phys. Paris Lett. *41*, L473 (1980);
H.W.J. Blöte, M.P. Nightingale, B. Derrida: J. Phys. A*14*, L45 (1981)
7.114 H.J. Hilhorst: Phys. Lett. *56*A, 153 (1976); Phys. Rev. B*16*, 1253 (1977)
7.115 T.C. Lubensky, C. Dasgupta, C.M. Chaves: J. Phys. A*11*, 2219 (1978)
7.116 A. Malakis: Physica *104*A, 427 (1980)
7.117 A. Baumgärtner: J. Phys. A*13*, L39 (1980)
7.118 A. Coniglio, M. Daoud: J. Phys. A*12*, L259 (1979)
7.119 M. Daoud, A. Coniglio: J. Phys. A*14*, L108 (1981)
7.120 J. Kertész, T. Vicsek: J. Phys. C*13*, L343 (1980)
7.121 P.J. Reynolds: Preprint (1981)
7.122 S. Redner: J. Phys. A*14*, L349 (1981);
S. Redner, A.C. Brown: J. Phys. A*14*, L285 (1981)
7.123 W. Kinzel, J. Yeomans: J. Phys. A*14*, L163 (1981)
7.124 W. Klein, W. Kinzel: J. Phys. A*14*, L405 (1981);
W. Klein: J. Phys. A*15* (1982)
7.125 S. Redner, Z.R. Yang: J. Phys. A*15*, 77 (1982)
7.126 S. Redner: Phys. Rev. B*25*, 3242 (1982)
7.127 S. Redner: Phys. Rev. B*25*, 5646 (1982)
7.128 H. Nakanishi, P.J. Reynolds, S. Redner: J. Phys. A*14*, 855 (1981);
H. Ikeda: Prog. Theor. Phys. *61*, 842 (1979)
7.129 A.C.N. de Magalhães, C. Tsallis, G. Schwachheim: J. Phys. C*14*, 1393 (1981)
7.130 C.M. Chaves, P.M. Oliveira, S.L.A. de Queiroz: Prog. Theor. Phys. *62*, 1550 (1979)
7.131 P. Murilo Oliveira: Phys. Rev. B*25* (1982)
7.132 P. Murilo Oliveira: Phys. Rev. Lett. *47*, 1423 (1981)
7.133 M. Napiórkowski, P.C. Hemmer: Phys. Lett. *76*A, 359 (1980)
7.134 M. Napiórkowski, P.C. Hemmer: Phys. Lett. *75*A, 153 (1980)
7.135 A. Gonzales, P.J. Reynolds: Phys. Lett. *80*A, 357 (1980)
7.136 H. Gould, F. Family, H.E. Stanley: Preprint (1982);
H.P. Peters, D. Stauffer, H.P. Hölters, D. Loewenich: Z. Phys. B*34*, 339 (1979)
7.137 H.E. Stanley, J. Teixeira: J. Chem. Phys. *73*, 3404 (1980)
7.138 C. Tsallis, G. Schwachheim: J. Phys. C*12*, 9 (1979);
C. Tsallis, S.V.F. Levy: J. Phys. C*13*, 465 (1980);
S.V.F. Levy, C. Tsallis, E.M.F. Curado: Phys. Rev. B*21*, 2991 (1980)
7.139 C. Tsallis: J. Phys. C*13*, L85 (1981);
F.C. Alcaraz, C. Tsallis: J. Phys. A*15*, 587 (1982)
7.140 H.E. Stanley: J. Phys. A*12*, L329 (1979)